

ARTIFICIAL PHOTOSYNTHESIS: DYE ASSISTED PHOTOCATALYTIC
REDUCTION OF CARBON DIOXIDE OVER PURE AND PLATINUM
CONTAINING TITANIA

A THESIS SUBMITTED TO
THE GRADUATE SCHOOL OF NATURAL AND APPLIED SCIENCES
OF
MIDDLE EAST TECHNICAL UNIVERSITY

BY

ÖZLEM ÖZCAN

IN PARTIAL FULFILLMENT OF THE REQUIREMENTS
FOR
THE DEGREE OF MASTER OF SCIENCE
IN
CHEMICAL ENGINEERING

JULY 2005

Approval of the Graduate School of Natural and Applied Sciences

Prof. Dr. Canan ÖZGEN
Director

I certify that this thesis satisfies all the requirements as a thesis for the degree of
Master of Science

Prof. Dr. Nurcan BAÇ
Head of Department

This is to certify that we have read this thesis and that in our opinion it is fully
adequate, in scope and quality, as a thesis for the degree of Master of Science

Prof. Dr. Engin AKKAYA
Co-Supervisor

Prof. Dr. Deniz ÜNER
Supervisor

Examining Committee Members

Prof. Dr. Timur DOĞU (METU, ChE) _____

Prof. Dr. Deniz ÜNER (METU, ChE) _____

Prof. Dr. Engin U. AKKAYA (METU, CHEM) _____

Prof. Dr. Şinasi ELLİALTIOĞLU (METU, PHYS) _____

Assoc. Prof. Dr. Oğuz GÜLSEREN (Bilkent Univ., PHYS) _____

I hereby declare that all information in this document has been obtained and presented in accordance with academic rules and ethical conduct. I also declare that, as required by these rules and conduct, I have fully cited and referenced all material and results that are not original to this work.

Name, Last name: Özlem ÖZCAN

Signature :

ABSTRACT

ARTIFICIAL PHOTOSYNTHESIS: DYE ASSISTED PHOTOCATALYTIC REDUCTION OF CARBON DIOXIDE OVER PURE AND PLATINUM CONTAINING TITANIA

Özcan, Özlem

M.S., Department of Chemical Engineering

Supervisor : Prof. Dr. Deniz Üner

Co-Supervisor: Prof. Dr. Engin U. Akkaya

July 2005, 65 pages

The aim of this study is to test the limits of photocatalytic reduction of CO₂ over Pt and light harvesting dye promoted TiO₂ films under UV and visible light. Thick and thin TiO₂ film catalysts are coated onto 1 cm long glass beads via a common sol-gel procedure and dip coating technique. TiO₂ thin films were promoted by Pt and three different light harvesting molecules: RuBpy (Tris (2,2' – bipyridyl) ruthenium (II) chloride hexahydrate) , BrGly (1,7-dibromo-N,N'-(t-butoxycarbonyl-methyl)-3,4:9,10-perylene-diimide) and BrAsp (1,7-dibromo-N,N'-(S-(1-t-butoxycarbonyl-2-t-butoxycarbonyl-methyl)-ethyl)- 3,4:9,10-perylenediimide). Their SEM, XRD, UV-Vis spectroscopy and hydrogen chemisorption characterizations are performed.

Reaction tests are performed for the catalysts under UV and visible light. The only quantifiable reaction product was methane. With RuBpy containing catalysts hydrogen production was observed under UV light, but not quantified. The results indicated that Pt addition resulted in higher yields in UV experiments. The presence

of light harvesting molecules resulted in increase in photocatalytic activity for thin films, whereas it resulted in no change or decrease for the thick films. The latter case may occur due to the UV filtering effect of these dyes.

Use of dyes (with visible range absorption bands) as promoters made visible light excitation possible. This resulted in photocatalytic activity under visible light, which was not observed with unpromoted and Pt promoted TiO₂ thin film catalysts. Under visible light methane was the only quantified photoreduction product. CO evolution was also observed, but not quantified. The photocatalytic activities of the dye promoted TiO₂ were in the order of RuBpy~BrAsp>BrGly. The methane yields of visible light experiments were one order of magnitude lower than the ones under UV light.

Keywords: Artificial photosynthesis, Carbon dioxide reduction, TiO₂ thin films, Visible light excitation

ÖZ

SUNİ FOTOSENTEZ: KARBON DİOKSİTİN SAF VE PLATİN İÇEREN TİTANYA ÜZERİNDE BOYA YARDIMIYLA FOTOKATALİTİK İNDİRGENMESİ

Özcan, Özlem

Yüksek Lisans, Kimya Mühendisliği Bölümü

Tez Yöneticisi : Prof. Dr. Deniz Üner

Ortak Tez Yöneticisi: Prof. Dr. Engin U. Akkaya

Temmuz 2005, 65 sayfa

Bu çalışmanın amacı carbon dioksitin Pt ve ışık hasatlayan moleküllerle kaplanmış TiO₂ filmler üzerinde UV ve görünür dalgaboylarındaki ışık altında fotokatalitik yollarla indirgenmesinin limitlerini incelemektir. İnce ve kalın TiO₂ film katlizörler 1 cm uzunluğundaki cam borulara sol-gel prosedürü ve daldırarak kaplama tekniği uygulanarak kaplanmıştır. TiO₂ filmler Pt ve RuBpy (Tris (2,2'-bipyridyl)ruthenium(II)chloride-hexahydrate) , BrGly (1,7-dibromo-N,N'-(t-butoxy-carbonyl-methyl)-3,4:9,10-perylene-diimide) ve BrAsp (1,7-dibromo-N,N'-(S-(1-t-butoxycarbonyl-2-t-butoxycarbonyl-methyl)-ethyl)-3,4:9,10-perylene-diimide) ışık hasatlayan molekülleri ile kaplanmıştır. Filmlerin SEM, XRD, UV-Vis spektroskopisi ve hidrojen kimyasal adsorplanması karakterizasyonları yapılmıştır.

Tepkime testleri UV ve görünür dalga boyunda ışık kullanılarak yapılmıştır. Miktarı hesaplanabilen tek tepkime ürünü metandır. RuBpy eklenmiş katalizörlerde

UV ışık altında hidrojen üretimi gözlenmiş ama miktarı hesaplanamamıştır. Sonuçlara göre, Pt eklenmesi UV dalgaboyundaki deneylerde aktivite artışına yol açmıştır. Işık hasatlayan moleküllerin kullanılması ince filmlerde UV ışık aktivitesinde artışa yol açarken kalın filmlerde bunun tersi gözlemlenmiştir. Bunun nedeninin bu moleküllerin UV dalgaboyundaki filtreleme özellikleri olduğu düşünülmektedir.

Görünür dalga boyunda ışık hasatlayan moleküllerin kullanılması görünür dalga boyundaki ışıkla elektron uyarılmasını mümkün kılmıştır. Bu da TiO_2 ve Pt eklenmiş TiO_2 katalizörlerinde gözlenemeyen, görünür ışık altında fotokatalitik aktiviteye yol açmıştır. Görünür dalgaboyundaki ışık altında da miktarı hesaplanabilen tek ürün metan olmuştur. CO oluşumu gözlenmiş ama miktarı hesaplanamamıştır. Boyaların TiO_2 fotokatalitik aktivitesi üzerindeki etkileri RuBpy~BrAsp>BrGly şeklindedir.

Anahtar Kelimeler: Suni fotosentez, Karbon dioksit indirgenmesi , TiO_2 ince filmler, Görünür dalgaboylarında uyarılma

To My Grandfather

ACKNOWLEDGMENTS

The author wishes to express her deepest gratitude to her supervisor Prof. Dr. Deniz Üner and co-supervisor Prof. Dr. Engin U. Akkaya for their guidance, advice, encouragements and support throughout this study.

The author would also like to thank CATALYSST Project Group for their suggestions and comments.

The author wishes to express her appreciation to her family, without their endless support the realization of her goals would not be possible.

The author would like to express her intimate thanks to Can Sandıkçiođlu for being there for her to share the life, for his encouragements and motivation.

Without the friends, working in the lab will not be this educative and pleasing. Therefore all former and current members of CaCTUS Research Group, Ela Erođlu, Zeynep ulfaz, Belma Soydař and all E-Building students deserve the greatest appreciation.

The technical assistance of Mrs. Kerime Güney, Mrs. Gülten Orakçı and Personnel of Chemical Engineering Machine Workshop are gratefully acknowledged.

This study was supported by the METU Institute of Natural and Applied Sciences Grant No: BAP-2004-07-02-00-100 and YUUP - Artificial Ecosystem.

TABLE of CONTENTS

PLAGIARISM.....	iii
ABSTRACT.....	iv
ÖZ.....	v
DEDICATION.....	vi
ACKNOWLEDGMENTS.....	vii
TABLE OF CONTENTS.....	x
LIST OF TABLES.....	xii
TABLE OF FIGURES.....	xiii
CHAPTER	
1. INTRODUCTION.....	1
2. LITERATURE SURVEY.....	6
2.1 CARBON DIOXIDE REDUCTION ON TiO ₂ CATALYSTS.....	8
2.2 SYNTHESIS AND PROMOTION OF TiO ₂ FILMS.....	11
2.3 DYE SENSITIZED SOLAR CELLS.....	14
3. MATERIALS AND METHODS.....	16
3.1 CATALYST PREPARATION.....	16
3.1.1 Thin Films	16
3.1.1.1 Transparent TiO ₂ films.....	16
3.1.1.2 Pt promoted TiO ₂ films.....	18
3.1.1.3 Light harvesting molecule (LHM) promoted TiO ₂ and Pt.TiO ₂ films.....	19
3.1.2 Thick Films	21
3.1.2.1 TiO ₂ thick films.....	21
3.1.2.2 Pt promoted TiO ₂ films.....	21

3.2 CATALYST CHARACTERIZATION	23
3.3 CATALYST TESTING	24
4. RESULTS AND DISCUSSIONS	26
4.1 CATALYST CHARACTERIZATION RESULTS.....	26
4.2 REACTION TEST RESULTS.....	26
4.2.1 Thin Films	27
4.2.1.1 UV Light Reaction Tests.....	27
4.2.1.2 Visible Light Reaction Tests.....	31
4.2.1 Thick Films	32
4.2.2.1 UV Light Reaction Tests.....	32
4.2.2.2 Visible Light Reaction Tests.....	37
4.2.1 Thin Films vs. Thick Films	44
5. CONCLUSIONS	47
6. RECOMMENDATIONS	49
REFERENCES.....	51
APPENDICES	
A. TGA DATA	56
B. SYNTHESIS PROCEDURES of LIGHT HARVESTING MOLECULES..	57
C. REACTION TEST RESULTS in TABULAR FORM.....	61
D. SEM IMAGES of THIN FILMS.....	63
E. PICTURE of REACTION TEST SETUP	65

LIST OF TABLES

Table 2.1 Carbon dioxide reduction reactions and their electropotentials.....	7
Table 3.1 Light harvesting molecules used in this study, their chemical formulas and molecular structures	20
Table 3.2 GC Operation Parameters	25
Table 4.1 UV-Vis Absorption maxima of TiO ₂ .RuBpy, TiO ₂ .BrGly and TiO ₂ . BrAsp.....	27
Table C.1 Thin Film Reaction Test Results	61
Table C.2 Thin Film Reaction Test Results	62

LIST OF FIGURES

Figure 1.1 Electromagnetic Spectrum and Corresponding Energies	2
Figure 2.1 Products of Sol-Gel method	13
Figure 3.1 Thin film coating procedure	17
Figure 3.2 Thick film coating procedure.....	22
Figure 3.3 Reaction Test Setup	24
Figure 4.1 Methane yields of TiO_2 , $\text{Pt}(\text{in}).\text{TiO}_2$ and $\text{Pt}(\text{on}).\text{TiO}_2$ thin film catalysts under UV light	28
Figure 4.2 Methane yields of TiO_2 , $\text{Pt}(\text{in}).\text{TiO}_2$, $\text{RuBpy}.\text{TiO}_2$ and $\text{RuBpy}.\text{Pt}(\text{in}).\text{TiO}_2$ thin film catalysts under UV light	29
Figure 4.3 Deactivation of $\text{RuBpy}.\text{Pt}(\text{in}).\text{TiO}_2$ catalyst under UV light during three consecutive test runs	30
Figure 4.4 Methane yields of $\text{RuBpy}.\text{Pt}(\text{in}).\text{TiO}_2$, $\text{BrGly}.\text{Pt}(\text{in}).\text{TiO}_2$ and $\text{BrAsp}.\text{Pt}(\text{in}).\text{TiO}_2$ thin film catalysts under visible light	31
Figure 4.5 Methane yields of TiO_2 , $\text{Pt}(\text{in}).\text{TiO}_2$ and $\text{Pt}(\text{on}).\text{TiO}_2$ thick film catalysts under UV light	33
Figure 4.6 Methane yields of $\text{RuBpy}.\text{TiO}_2$, $\text{BrGly}.\text{TiO}_2$, $\text{BrAsp}.\text{TiO}_2$ and TiO_2 film catalysts under UV light	34
Figure 4.7 Methane yields of TiO_2 , $\text{RuBpy}.\text{TiO}_2$, $\text{RuBpy}.\text{Pt}(\text{in}).\text{TiO}_2$ and $\text{RuBpy}.\text{Pt}(\text{on}).\text{TiO}_2$ thick film catalysts under UV light	35
Figure 4.8 Methane yields of TiO_2 , $\text{BrGly}.\text{TiO}_2$, $\text{BrGly}.\text{Pt}(\text{in}).\text{TiO}_2$ and $\text{BrGly}.\text{Pt}(\text{on}).\text{TiO}_2$ thick film catalysts under UV light.....	36
Figure 4.9 Methane yields of TiO_2 , $\text{BrAsp}.\text{TiO}_2$, $\text{BrAsp}.\text{Pt}(\text{in}).\text{TiO}_2$ and $\text{BrAsp}.\text{Pt}(\text{on}).\text{TiO}_2$ thick film catalysts under UV light	37
Figure 4.10 Methane yields of $\text{RuBpy}.\text{TiO}_2$, $\text{BrGly}.\text{TiO}_2$ and $\text{BrAsp}.\text{TiO}_2$ thick film catalysts under visible light	39

Figure 4.11 Methane yields of RuBpy.TiO ₂ , RuBpy.Pt(in).TiO ₂ and RuBpy.Pt(on).TiO ₂ thick film catalysts under visible light.....	40
Figure 4.12 Methane yields of BrGly.TiO ₂ , BrGly.Pt(in).TiO ₂ and BrGly.Pt(on).TiO ₂ thick film catalysts under visible light.....	41
Figure 4.13 Methane yields of BrAsp.TiO ₂ , BrAsp.Pt(in).TiO ₂ and BrAsp.Pt(on).TiO ₂ thick film catalysts under visible light	42
Figure 4.14 Methane yields of RuBpy.Pt(on).TiO ₂ , BrGly.Pt(on).TiO ₂ and BrAsp.Pt(on).TiO ₂ thin film catalysts under visible light	43
Figure 4.15 Comparison of methane yields of thick and thin films under UV light.....	44
Figure 4.16 Comparison of methane yields of thick and thin films of LHM.Pt(in).TiO ₂ catalysts under visible light.....	45
Figure 4.17 Comparison of methane yields per coated bead of thick and thin films under UV light.....	46
Figure B.1 Synthesis of 1,7-dibromo-3,6:9,10-perylenetetracarboxylic acid dianhydride	57
Figure B.2 Synthesis of 1,7-dibromo-N,N'-(<i>t</i> -butoxycarbonylmethyl)-3,4:9,10-perylene-diimide	58
Figure B.3 Synthesis of 1,7-dibromo-N,N'-(S-(1- <i>t</i> -butoxycarbonyl-2- <i>t</i> -butoxycarbonyl-methyl)-ethyl)-3,4:9,10-perylenediimide	60
Figure D.1 SEM images of the thin films (x500) a) TiO ₂ b) RuBpy.TiO ₂ c) Pt.TiO ₂ d) RuBpy.Pt.TiO ₂	63
Figure D.2 SEM images of the thin films (x5000) a) TiO ₂ b) RuBpy.TiO ₂ c) Pt.TiO ₂ d) RuBpy.Pt.TiO ₂	64
Figure E.1 Reaction Test Setup.....	65

CHAPTER I

INTRODUCTION

Large scale carbon dioxide emission to the atmosphere is one of the most important problems of today's industry. The control of carbon dioxide emissions via fixation or reduction is one of the attractive research fields. The fixation of carbon dioxide into storage materials can solve the problem only temporarily. A permanent solution can only be realized by reducing carbon dioxide to other compounds like hydrocarbons. Moreover, reduction of carbon dioxide to hydrocarbons or even to carbon monoxide is not only desirable to weaken the green house effect but also to create a renewable energy source.

The reduction of carbon dioxide to higher, more energetic hydrocarbons is a very energy demanding reaction due to the thermodynamically low energy content of carbon dioxide. Its activation is not possible under mild conditions at room temperature and atmospheric pressure. Available carbon dioxide reduction or reforming reactors operate at high temperatures and pressures. To design a feasible system, the energy for the reduction reactions have to be supplied without creating more carbon dioxide, which means not via burning of fossil fuels. At this point, utilization of the abundant solar energy appears to be a good alternative. Since the mechanism of energy transfer is excited state electron transfer in photocatalytic carbon dioxide reduction systems, they can operate under mild reactor conditions and do not require high temperatures and pressures.

For the design of artificial photosynthetic systems there are many challenges to be overcome. The most important challenge is in the field of material selection and preparation. There are many semiconductor materials with proven photocatalytic properties. Among them, TiO_2 , CdS , WO_3 , ZnO , SiO_2 , SrTiO_3 and

SiC can be listed. The reason for using semiconductor materials as photocatalysts is that they possess a band gap between their conduction and valence bands and this allows excitation to take place under irradiation. The electron at the excited state, which contains high amount of energy, is injected from the valence band to the conduction band, where it is mobile and ready to be used for catalytic reactions.

The supply of energy from the Sun to Earth reaches 3×10^{24} Joules a year, which is ~ 10000 times more than the current annual global power consumption. Most of the semiconductor materials mentioned previously, possess wide band gaps; therefore UV light is necessary for the excitation of electrons. However, due to the presence of the protective ozone layer just 4% of this energy flow is in form of UV light, which contains higher energy per photon.

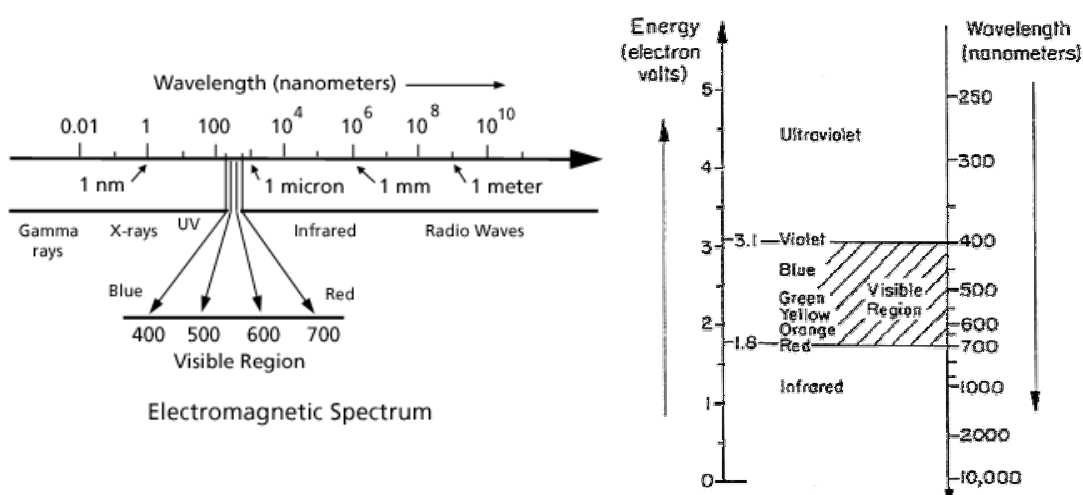


Figure 1.1 Electromagnetic Spectrum and Corresponding Energies

The ultimate aim of this study is to design a catalyst that can operate with solar light, so that an additional light source will not be necessary. As seen from Figure 1.1 above, the energy of visible light is between 1.8 and 3.1 eV, where the red light with 700 nm has the lowest, and violet light with 400 nm has the highest

energy values. To be able to design a system operating with visible light the photocatalytic material has to possess a narrower band gap, which can be overcome with photons of energy in the range of 1.8 to 3.1 eV.

In addition to the photocatalytic properties, the successful candidate for a global scale catalyst has to be a non-toxic, inexpensive, stable and widely available material. Considering all these criteria, scientists have mainly focused on TiO₂ based systems since 1980's. TiO₂ has a band gap of 3.2 eV [1]. Therefore, great effort has been paid to shift this band gap to lower values by doping with various metal atoms such as Pt, Ag, W, Ru, Cu etc. or using advanced synthesis and after treatment techniques.

Another possibility of generating a visible light active TiO₂ catalyst is to combine TiO₂ with an organic dye, which can be excited with visible light. This concept is successfully applied by Graetzel to "Dye Sensitized Solar Cells" also known as Graetzel Cells and to photo-electrochemical water splitting cells [2]. Those solar cells use a dye anchored to a layer of TiO₂ as anode, a metal cathode and a suitable electrolyte, usually (I³⁻/I⁻). In such devices, the dye absorbs visible light, exciting an electron. The excited state electron is transferred to the conduction band of TiO₂ where it travels to the conduction glass electrode. The electron then flows through an external circuit and loads the cathode. At last, on the cathode, the electron reduces the oxidant (I³⁻) in the electrolyte. The reductant (I⁻) travels to the anode and regenerates the dye molecule. For those redox reactions, the respective energy levels of excited states and the energy levels of highest occupied valence band states and lowest unoccupied conduction band states of the semiconductors play an important role. The excitation band of the dye has to match with the conduction and valence band energy levels of the semiconductor, to be able to inject an electron at excitation and to be able to regenerate itself.

In this study, a similar approach is utilized for gas phase carbon dioxide reduction. Three different dyes have been loaded on TiO₂ and Pt-TiO₂ films and their photocatalytic activities for carbon dioxide reduction have been measured by analyzing the reaction products. The difference of the dye sensitized solar cells and

the system in this study is that, the redox mechanism in this study does take place on the same catalyst surface. The reduction of carbon dioxide takes place on a site with excited electron on the conduction band whereas the hole-site on the valence band oxidizes water to molecular oxygen completing the redox cycle.

For semiconductor photocatalysis, another challenge is to prevent the electron-hole recombination or charge recombination phenomena, which decreases the efficiency of the process. In general, an excited state molecule can undergo relaxation via three mechanisms: Fluorescence (back radiation), heat release (internal conversions) or electron transfer. The excitation takes place very rapidly on the order of $\sim 10^{-15}$ s. The relaxation processes occur at much slower rates. Heat release and fluorescence have lifetimes of $\sim 10^{-12}$ s and $\sim 10^{-7}$ s, respectively. Electron transfer to the adsorbed species is an even slower pathway. Since the excited state molecules prefer the pathway minimizing the excited state lifetime, the electron transfer steps are facing stiff competition. The addition of metal atoms into the TiO_2 framework also serves to the charge separation on the TiO_2 surface by pulling the excited state electron, hereby also physically separating the electron from the hole on the valence band.

Another challenge in realizing artificial photosynthesis systems is to utilize the sunlight efficiently. It has been reported that powdered catalysts have lower activities than the film catalysts due to scattering of light. The ideal system has to provide perfect contact of photocatalyst and light facilitating absorption of light. For both dye sensitized solar cells and other photocatalytic systems to increase the efficiency of the catalyst, or in other words, to maximize the “photocurrent” or “moles of product” per mass of photocatalytic material, thin films have been used. The synthesis of thin films is another attractive area of research. For TiO_2 thin films the most widely utilized synthesis technique is the sol-gel method, where a titanium containing organic precursor is mixed with a solvent and some amount of acid and hydrolyzed slowly upon addition of water. The water amount is controlled so that the gellation is retarded until the coating onto glass is established. Metal addition is

either done with TiO₂ coating or afterwards via aqueous solutions or in some studies via vapor deposition.

There are mainly two alternatives for the reaction system design. First route is using catalysts in a form of suspension in a solvent. The other one is to feed the reactants in gas phase and to use a heterogeneous system. The former one has the difficulty in choosing the proper solvent which will have no quenching properties and in which carbon dioxide will have high solubility. For the gas phase systems the lack of a carrier fluid creates a problem especially for multi-electron transfer reactions. Additionally, the separation of the products is a challenge for both systems.

Given the background and the constraints above, the objective has been set to test the gas phase photoreduction ability of dye promoted pure and Pt containing TiO₂.

CHAPTER II

LITERATURE SURVEY

The utilization of solar energy in photocatalytic reactions is a key research area in today's science world. The term "photocatalysis" is defined as photogeneration of a catalyst from an inert substrate [3]. For a process to be truly photocatalytic, the molecule at the excited state should not lose its excitation for infinite number of steps. A more general term is "photoinduced electron transfer catalysis", which has three types only two of them being truly photocatalytic:

Class 1 of Photoelectron-Transfer Catalysis:

In these reactions, electron transfer occurs as an initiating step, which is followed by a chain reaction where no termination steps exist. For this type of the catalysis the source of the photocatalyst is the substrate itself.

Class 2 of Photoelectron-Transfer Catalysis:

In this class, an inert substrate in the reaction medium is activated by light and catalyses a chain reaction where it does not lose its excited state, since the chain has no termination step. The difference between Class 1 and Class 2 is that in Class 2 the catalyst material is not one of the reagents.

Class 3 of Photoelectron-Transfer Catalysis:

In this class of photoelectron-transfer catalysis, a photosensitizer at its excited state, gives (or takes) an electron to (from) a substrate, which results in chemical activation of the substrate. This molecule then undergoes transformations and new products are formed. During these transformations, in one of the reaction steps, the photosensitizer regains its electron, however the electron is at its ground

state and the molecule needs another excitation to start the cycle over again. The reaction consumes photons and therefore is not a photocatalytic reaction. Most of the catalytic reactions, where the initiation step is an electron transfer process, can be catalyzed by photoinduced electron transfer catalysis at milder conditions.

Artificial photosynthesis reactions belong to the 3rd class of photoinduced electron transfer reactions, since they consume photons. In Table 1.1 below, reduction reactions to single carbon species, water splitting reaction and their electropotentials are shown.

Table 2.1 Carbon dioxide reduction reactions and their electropotentials [4]

Reaction	E/V vs. SHE	Electrons involved
$O_2 + 4 H^+ + 4 e^- \rightarrow 2 H_2O$	+ 0.82	4 e ⁻
$CO_2 + 2 H^+ + 2 e^- \rightarrow HCOOH$	- 0.61	2 e ⁻
$CO_2 + 2 H^+ + 2 e^- \rightarrow CO + H_2O$	- 0.52	2 e ⁻
$CO_2 + 4 H^+ + 4 e^- \rightarrow HCHO + H_2O$	- 0.48	4 e ⁻
$CO_2 + 6 H^+ + 6 e^- \rightarrow CH_3OH + H_2O$	- 0.38	6 e ⁻
$CO_2 + 8 H^+ + 8 e^- \rightarrow CH_4 + 2 H_2O$	- 0.24	8 e ⁻

The most widely used photocatalytic material in the literature is TiO₂ due to its high availability, low cost and non-toxicity. TiO₂ based photocatalysts can serve the environment by degrading dilute pollutants in air and water with oxidation reactions [5-11]. They can catalyze water splitting [12-14] as in the pioneering studies of Inoue et al. [15]. Moreover, it is possible to reduce the green house gases,

carbon dioxide and water to valuable products like methane or methanol over TiO₂ based catalysts [16-26].

2.1 CARBON DIOXIDE REDUCTION ON TiO₂ CATALYSTS

The reduction of carbon dioxide and water is not only important to decrease the amount of green house gases in the atmosphere but also to convert the available solar energy to chemical bond energy. The reduction products, like methane or methanol can be fed either to combustors or direct methanol fuel cells, where their oxidation will produce carbon dioxide and water. There are other methods for converting carbon dioxide to hydrocarbons like various reformers; however they require high temperatures and pressures, namely high energy input to activate the low energy containing carbon dioxide. The conventional energy production processes mainly involve combustion and therefore produce carbon dioxide. The required energy input has to be provided without generating further carbon dioxide. At this point the utilization of abundant solar energy is a good alternative and worth considering.

The research on photocatalytic reduction of carbon dioxide and water on TiO₂ based catalysts can be divided into two groups: liquid phase systems and gas phase systems. A wide range of promoters and dyes, also various synthesis methods have been tried to increase photocatalytic activity of TiO₂ and to shift its absorption band to visible region.

The groups working with liquid phase systems use TiO₂ catalysts as suspension in water. Among them, Solymosi and Tombácz [21] have worked on the effect of Rh deposition and W⁶⁺ doping on the photocatalytic performance of plain TiO₂ catalysts. Their results showed that Rh deposition resulted in increase of the photolysis yield and W⁶⁺ doping increased the electron concentration of TiO₂ and thereby enhanced the production and selectivity of formaldehyde production. The performance of Cu promoted TiO₂ catalysts has been investigated by Tseng and coworkers [19, 22, 23]. Their experiments showed that addition of copper resulted in

higher activity and those catalysts selectively produced methanol in presence of NaOH in the solution. The OH⁻ ions in the solution served as hole-scavengers and formed reactive OH radicals and also the presence of NaOH resulted in higher carbon dioxide solubility, which explains the high methanol yields and selectivity. They have also investigated the effect of synthesis procedures on the photocatalytic performance of sol-gel derived Cu/TiO₂ catalysts by using different Cu precursors. They have observed that CuCl₂ addition at the 0th hour of hydrolysis resulted in the best performance. The authors claim that this increased photocatalytic activity is due to the positive surface charge of this catalyst, which increased the carbonate adsorption and also the Cu-TiO₂ interaction.

According to Tseng and Wu [22], the possibility of carbon dioxide reduction depends on the energy position of the conduction band, ECB. The redox potential of carbon dioxide reduction to methanol is reported as -0.62 eV. The ECB of anatase TiO₂ is -0.75 eV. Therefore, in case of excitation with light, TiO₂ is able to donate an electron to carbon dioxide and catalyze its reduction. The result that the metal loading increases the activity of TiO₂ is observed, because the addition of metal atoms decreases the electron-hole recombination probability by causing charge separation. Tseng and Wu illustrate this by comparing Cu/TiO₂ with Ag/TiO₂. The redox potentials of Cu²⁺/Cu⁺ and Cu⁺/Cu⁰ are 0.1 eV and 0.5 eV, respectively, whereas that of Ag⁺/Ag⁰ is nearly 0.8 eV. Therefore the photogenerated electrons are transferred both to Cu and Ag sites, however the electrons transferred to Cu have the chance to be transferred further to the adsorbates, whereas the ones transferred to Ag are trapped there because of the positively high redox potential. This explains the lower yields of Ag promoted catalysts versus the Cu promoted ones.

The gas phase studies are usually done in reaction cells connected to vacuum lines by feeding desired amounts of carbon dioxide and water vapor to the cell. Many reports have been written by Anpo and his coworkers on gas phase photo reduction of carbon dioxide over various TiO₂ containing catalysts. Among them are TiO₂ containing zeolites, mesoporous molecular sieves, silica thin films and Ti-MCM-41 and Ti-MCM-48 catalysts [16, 17, 18, 20, 24, 25]. The catalysts

synthesized by addition of TiO₂ into the zeolites cavities were more active than the pure anatase TiO₂ powder [20]. Yamashita et al. have reported that methanol production is observed the tetrahedrally coordinated Ti-oxide species, where as bulk titania and octahedrally coordinated Ti-oxide catalysts preferred methane production. Additionally, the effect of Pt addition is investigated by Yamashita and coworkers and it is reported that in the presence of Pt methane production is favored and the highest yields have been observed. This increase in methane yields due to metal addition is in agreement with the results of Tseng et al.'s studies, mentioned above. The methane selectivity is claimed to occur due to the charge separation. Since there is no liquid media to transfer additional OH radicals to the reduction sites, the carbon species adsorbed on the electron-sites are in contact with co-adsorbed H radicals and this leads to formation of methane instead of methanol. Also on the Ti-MCM-41 and Ti-MCM-48 catalysts similar results are obtained [16]. The same behavior, namely methane selectivity is observed upon addition of Pt to the catalysts as in the zeolite catalysts. However there was no significant change in the photocatalytic performance of the catalyst.

Lin and coworkers [26] studied the reduction mechanism of carbon dioxide and water by in-situ FTIR. The catalyst used was Ti-MCM-41, the sole carbon-product was CO and O₂ evolution is observed. By using D₂O, ¹³CO₂ and C¹⁸O₂ they were able to identify that H₂O is the stoichiometric electron donor. This work reports that CO is a single-photon, 2-electron-transfer product.

The effect of the hydrophobic and hydrophilic properties of Ti-β zeolite catalysts is investigated by using different structure directing agents (SDA's), one containing OH⁻ ions and another one containing F⁻ ions [25]. The zeolite synthesized with the former SDA is hydrophilic whereas the latter one results in a hydrophobic surface. Ikeue and coworkers [25] claimed that the competitive interaction of CO₂ and H₂O with the excited sites result in C, H and OH radicals and those radicals react to form methane and methanol molecules. The interaction of H₂O and the surface is limited due to the hydrophobic nature of the F containing catalysts, which results in lower yields but higher methanol selectivities. This showed that the

photocatalytic performance of a catalyst is also dependent on the hydrophilic or hydrophobic properties of the material.

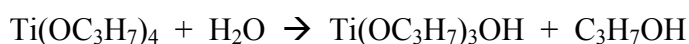
So far both the liquid and gas phase studies were utilizing TiO₂ catalysts in powder form. An alternative approach is to use TiO₂ as a thin film. Ikeue et al. [17, 18, 24] studied the photocatalytic performance of Ti-containing porous silica thin films. The yields obtained with film catalysts were higher than that ones obtained on powder catalysts with same composition and also higher than Ti-MCM-48 catalysts, which is attributed to their transparency. Also different H₂O/CO₂ ratios have been tried to see the effect of surface OH concentration on the methanol selectivity. It was observed that by increasing this ratio the surface OH groups are occupied with H₂O molecules and the selectivity towards methane is increased. A low H₂O/CO₂ ratio is claimed to prevent methane formation.

2.2 SYNTHESIS AND PROMOTION OF TiO₂ FILMS

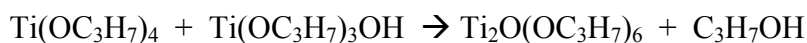
In recent years, the research on semiconductor photocatalysis mainly focused on TiO₂ thin films, instead of powdered TiO₂ photocatalysts. The reason is that TiO₂ thin films scatter less light than the powdered catalysts. Those thin titania films are tested both for oxidation and reduction reactions. The application areas vary from degradation of organic pollutants in air and water to water splitting, from carbon dioxide reduction to NO_x reduction [27, 29-36].

The synthesis of TiO₂ films is an attractive area of material science. Different techniques are applied to synthesize TiO₂ films that possess high surface area, high photocatalytic activity and stability. Most widely utilized technique is the sol-gel method. The sol-gel method involves the controlled polymerization of a metal-alkoxide solution. When the solvent is evaporated the void spaces in the structure result in a high surface material. The polymerization reactions are as follows [34]:

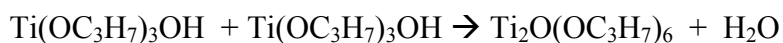
1. Hydrolysis



2. Condensation



3. Water Condensation



Those condensation reactions lead to Ti-O-Ti bonds, which then construct the TiO₂ network. Also the OH end of hydrolysed titanium isopropoxide is making the attachment to the glass surface possible. The role of the acid in the sol-gel technique is firstly that it catalyses the hydrolysis reactions and secondly that acids react with alcohols in a esterification reaction releasing water. This slow water production also helps to control the water ratio and hereby gellation of the sol.

Many different products can be synthesized with sol-gel procedure. The structure of the product can be determined by water to alkoxide ratio and the after treatment methods. Figure 2.1 summarizes the sol-gel products, which can be obtained using different treatment techniques.

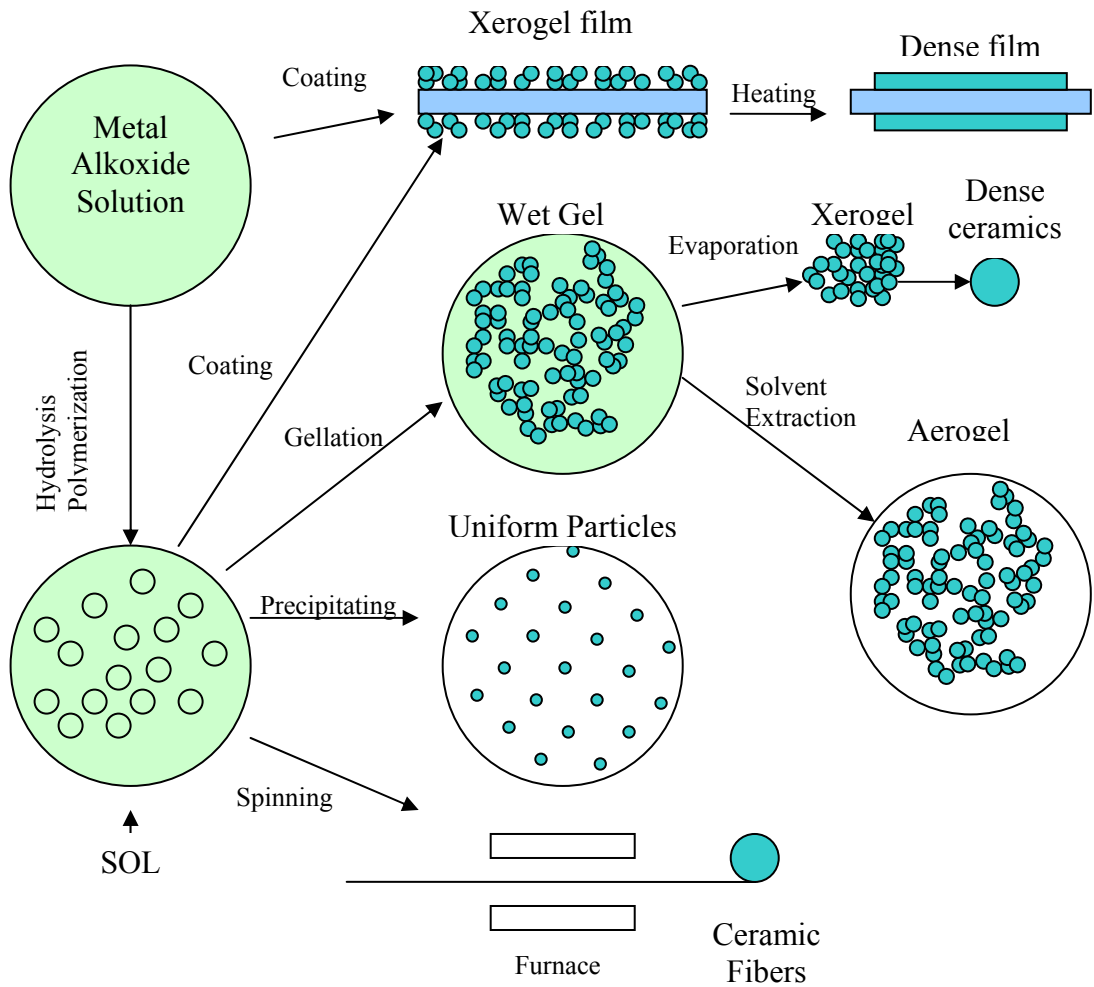


Figure 2.1 Products of Sol-Gel method [28]

The preparation of TiO_2 films is done via the coating of prepared sol onto glass substrates as illustrated in Figure 2.1 above. TiO_2 has two crystalline forms, anatase and rutile. The bandgaps of anatase and rutile are 3.23 eV (384 nm) and 3.02 eV (411 nm) respectively. Anatase is proven to be photocatalytically more active than the rutile for most of the reactions [37].

To increase the photocatalytic activity of TiO_2 films metal addition is used. The metal addition is done in various ways. Among them are photodeposition, deposition-precipitation [23], impregnation [16, 19, 23], and mixing to the prepared sol [22]. The amount of the metal added to the TiO_2 catalyst is important since the

surface aggregation or sintering plays an important role in determination of electronic properties of the catalyst.

The similar coating techniques are also applied to solar cell electrodes. Conducting glass or metal electrodes are coated with TiO₂ to produce photo-excitabile electrodes [2, 38, 39, 40]. For solar cells many ligands have been tried to be coated onto TiO₂ surface to make visible light excitation possible [41].

2.3 DYE SENSITIZED SOLAR CELLS

Dye sensitized solar cells consist of a visible light active dye anchored to a layer of TiO₂ as anode, a metal cathode and a suitable electrolyte in many studies I³⁻/I). The working mechanism of the solar cells starts with the absorption of visible light by the dye, exciting an electron. This electron at its excited state is then transferred to the conduction band of TiO₂ in which it travels to the conduction glass electrode. After it reaches the external circuit the electron then loads the cathode. At last, on the cathode surface, the electron reduces the oxidant (I³⁻) present in the electrolyte. The reductant (I) travels to the anode and regenerates the dye molecule. For those redox reactions, the respective energy levels of excited states and the energy levels of highest occupied (HOMO) and lowest unoccupied (LUMO) orbitals of the semiconductors have to match. The HOMO-LUMO energy levels of the dye has to match with the conduction band and valance band energy levels of the semiconductor to be able to inject an electron after excitation and to be able to regenerate itself at the end of one redox cycle.

Dye sensitized solar cells are developed as an alternative to the conventional solid-state p-n junction photovoltaics like silicon wafer solar cells for the direct conversion of solar energy into electricity. The direct use of coordination compounds, such as [Ru(Bpy)₃]₂⁺, as light harvesting molecule in homogeneous cells resulted in photocurrent responses, however with low efficiencies due to the fast recombination of the photoproducts in the solution [41].

The use of wide band-gap semiconductors required UV or near UV light to create electron–hole pairs. Although the anchoring of light harvesting molecules was restricted by the surface area of TiO₂, this combination resulted in advantages over direct band to band excitation of semiconductors due to the reduction of electron–hole recombination [2].

Semiconductors in mesoporous membrane type film with a high surface area led to an efficient light absorption by attached sensitizers. Solar cells employing such photoanodes presented promising results, with photoresponse 1000 times higher for the nanostructured electrode [42]. Regenerative photoelectrochemical solar cells based on a thin-layer sandwich-type set-up containing a dye-sensitized nanocrystalline TiO₂ photoanode are now commercially feasible devices [2, 41].

Dye sensitization of semiconductor materials has resulted in a successful solution to extending the absorption capability of the cells to visible light with promising results. This approach is advantageous over the direct semiconductor excitation in conventional solar cells, since attached dyes, rather than the semiconductor itself, are the light absorbing material. So, the processes of light absorption and charge transfer are separated by the semiconductor-sensitizer interface lowering the probability of electron–hole recombination [41, 43].

Electron injection from the photoexcited light harvesting molecule into the conduction band of the semiconductor occurs with an energy lower than the band gap of the semiconductor, providing good sunlight harvesting by sensitizers (dyes). A good photosensitizer should possess intense absorption capacity in the visible region, strong adsorption capability onto the semiconductor surface and a high electron injection efficiency into the conduction band of the semiconductor. Moreover, the light harvesting molecule must easily regenerate itself by the electrolyte in order to prevent electron recombination processes and be sufficiently stable. Many different compounds have been investigated for semiconductor sensitization, such as porphyrins, pyridines, coumarin and figgerent transition metal complexes [41, 44-49].

CHAPTER III

MATERIALS AND METHODS

3.1 CATALYST PREPARATION

Thin and thick films of promoted and unpromoted TiO₂ are prepared using following precursor sols. Films are coated on 1 cm long, 6 mm OD glass beads, using dip coating technique. For XRD and SEM analysis, 1 mm thick microscope glasses are coated using the same procedures. For BET and TGA analysis powdered TiO₂ catalyst was prepared by allowing the sol to undergo gellation and by applying the same calcination procedure.

3.1.1 Thin Films

For thin film preparation tetra isopropyl orto titanate (Merck) was used as Ti source. Isopropanol, acetic acid and water are used as solvent, modifier and hydrolyser respectively. Water amount is very important for sol-gel synthesis technique since it determines the gellation time. The synthesis procedure requires the sol to be stable, i.e. not to gellate, at least for six hours. To determine the best recipe, which would be stable during the whole procedure, many water to tetra isopropyl orto titanate ratios were tried and the proper one was selected and used throughout the study.

3.1.1.1 Transparent TiO₂ films

The sol for TiO₂ coating was prepared by mixing tetra isopropyl orto titanate, isopropanol, acetic acid and water with following ratio [6 : 120 : 2.5 : 1]. To obtain a

more stable sol, water and acetic acid was firstly mixed with half volume of required isopropanol and added to the tetra isopropyl ortho titanate-isopropanol mixture afterwards. Addition was done slowly and the mixture was stirred continuously to provide a good mixing and to prevent local gellation.

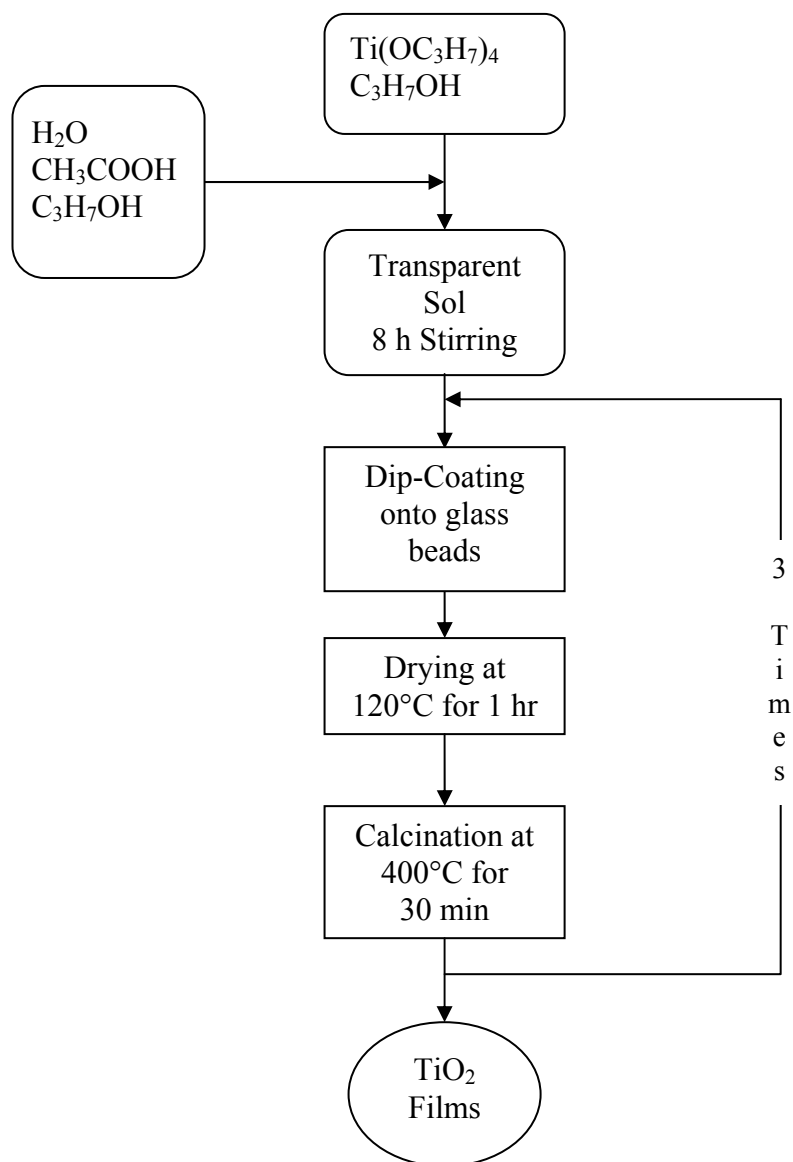


Figure 3.1 Thin film coating procedure

The coating was established by dipping the beads into the sol with a dipping rate of 7.5 cm/min, waiting for 10 minutes and pulling them with the same speed. The beads are then dried at 120°C in air in a furnace. They are then calcined at 400°C for 30 minutes. This procedure was repeated for three times for a successful coating.

3.1.1.2 Pt promoted TiO₂ films

To synthesize Pt promoted TiO₂ films, Pt(NH₃)₄Cl₂·H₂O (Johnson Matthey) was used as Pt source. Two types of Pt promoted films, Pt(on) and Pt(in) films, are prepared to see the effect of Pt addition procedure on the photocatalytic performance of the films. Pt(on) catalysts are prepared using aqueous solutions of Pt containing salt and Pt was added on a TiO₂ support via wet impregnation technique. On the other hand for Pt(in) catalysts Pt salt was added to the TiO₂ coating sol, so that Pt was added to TiO₂ framework.

a) Pt(on) Catalysts

To prepare Pt(on) catalysts an appropriate amount of salt was dissolved in water and coated onto previously prepared TiO₂ films. The amount of the salt was adjusted in such a way that its solution will contain 1 mole of Pt for 1000 moles of Ti for same volume of solution. So the concentration was 0.1% Pt/Ti. For annealing and calcination same cycles are applied as in TiO₂ coating. The coating was established by dipping the beads into the solution with a dipping rate of 7.5 cm/min, waiting for 10 minutes and pulling them with the same speed. The beads are then dried at 120°C in air in a furnace. They are then calcined at 400°C for half an hour. This procedure was repeated for three times for a successful coating.

b) Pt(in) Catalysts

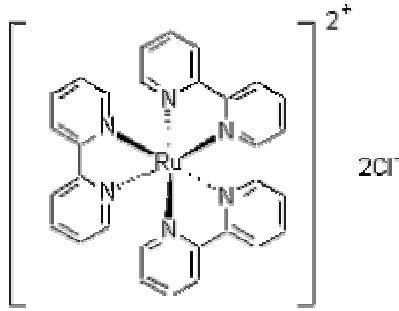
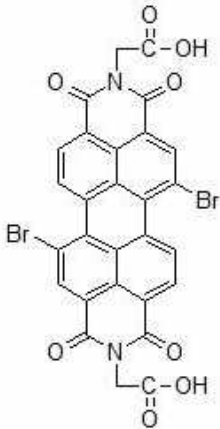
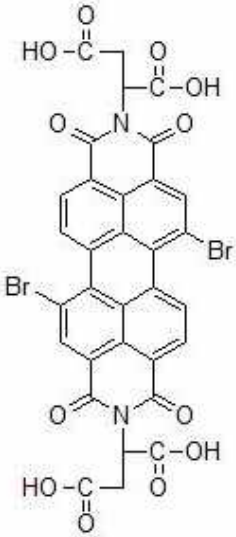
To prepare Pt(in) catalysts Pt salt was added to TiO₂ coating sol with the same 1 mole of Pt for 1000 moles of Ti ratio. The coated beads are annealed and calcined according to the same procedure as in TiO₂ coating. The coating was established by dipping the beads into the sol with a dipping rate of 7.5 cm/min, waiting for 10 minutes and pulling them with the same speed. The beads are then dried at 120°C in air in a furnace. They are then calcined at 400°C for half an hour. This procedure was repeated for three times for a successful coating.

3.1.1.3 Light harvesting molecule (LHM) promoted TiO₂ and Pt-TiO₂ films

Three different light harvesting molecules were used in this study: Tris(2,2'-bipyridyl)ruthenium(II)chloride-hexahydrate, which is abbreviated as RuBpy; 1,7-dibromo-N,N'-(t-butoxy-carbonyl-methyl)-3,4:9,10-perylene-diimide, which is abbreviated as BrGly and 1,7-dibromo-N,N'-(S-(1-t-butoxy-carbonyl-2-t-butoxycarbonyl-methyl)-ethyl)-3,4:9,10-perylenediimide, which is abbreviated as BrAsp. Their molecular structures were given in Table 3.1. RuBpy was purchased from Aldrich Chemicals. BrGly and BrAsp have been synthesized in Prof. Dr. Engin Akkaya's laboratory, in Chemistry Department, METU by Funda Yükrük[50]. The synthesis procedures for BrGly and BrAsp are given in Appendix B, with the intention of collecting all related information in one volume.

Appropriate amount of LHM was dissolved in water. For dissolving BrGly and BrAsp in water small amount of NaHCO₃ salt was added. The coating was established by dipping the beads into the solution with a dipping rate of 7.5 cm/min, waiting for 10 minutes and pulling them with the same speed. The beads are then dried at 120°C in air in a furnace. LHM promoted catalysts are not calcined to prevent the decomposition of organic dyes.

Table 3.1 Light harvesting molecules used in this study, their chemical formulas and molecular structures

Abbreviation	Chemical Formula	Molecular Structure
RuBpy	Tris (2,2' – bipyridyl) ruthenium (II) chloride hexahydrate	
BrGly	1,7-dibromo-N,N'-(t-butoxycarbonylmethyl)-3,4:9,10-perylene-diimide	
BrAsp	1,7-dibromo-N,N'-(S-(1-t-butoxycarbonyl-2-t-butoxycarbonyl-methyl)-ethyl)-3,4:9,10-perylenediimide	

3.1.2 Thick Films

Thick films have been synthesized to see whether the catalyst bed can be scaled up by coating more catalyst onto the beads instead of using much more beads with thin coating. For thick film preparation tetra isopropyl ortho titanate was used as Ti source. Ethanol, acetic acid and water are used as solvent, modifier and hydrolyser respectively.

3.1.2.1 TiO₂ thick films

The sol for TiO₂ coating was prepared by mixing tetra isopropyl ortho titanate, ethanol, acetic acid and water with following volumetric ratio [14.2 : 18.4 : 0.24 : 0.5]. The coating was established by dipping the beads into the sol with a dipping rate of 7.5 cm/min, waiting for 10 minutes and pulling them with the same speed. The beads are then dried at 120°C in air in a furnace. They are then calcined at 400°C for half an hour. This procedure was repeated for three times for a successful coating.

The coating procedure was summarized in Figure 3.2.

3.1.2.2 Pt promoted TiO₂ films

To synthesize Pt promoted TiO₂ films, Pt(NH₃)₄Cl₂·H₂O was used as Pt source. As in the thin film section two types of Pt promoted films were prepared. The same nomenclature was used for the thick films as well. Pt(on) catalysts refer to the catalysts prepared using aqueous solutions of Pt salt and thus Pt is added on TiO₂ support. The name “Pt(in)” refers to the catalysts coated with Pt salt added sol, so that Pt is added to TiO₂ structure. Pt and LHM addition procedures in 3.1.1.2 and 3.1.1.3 were exactly repeated for thick films as well.

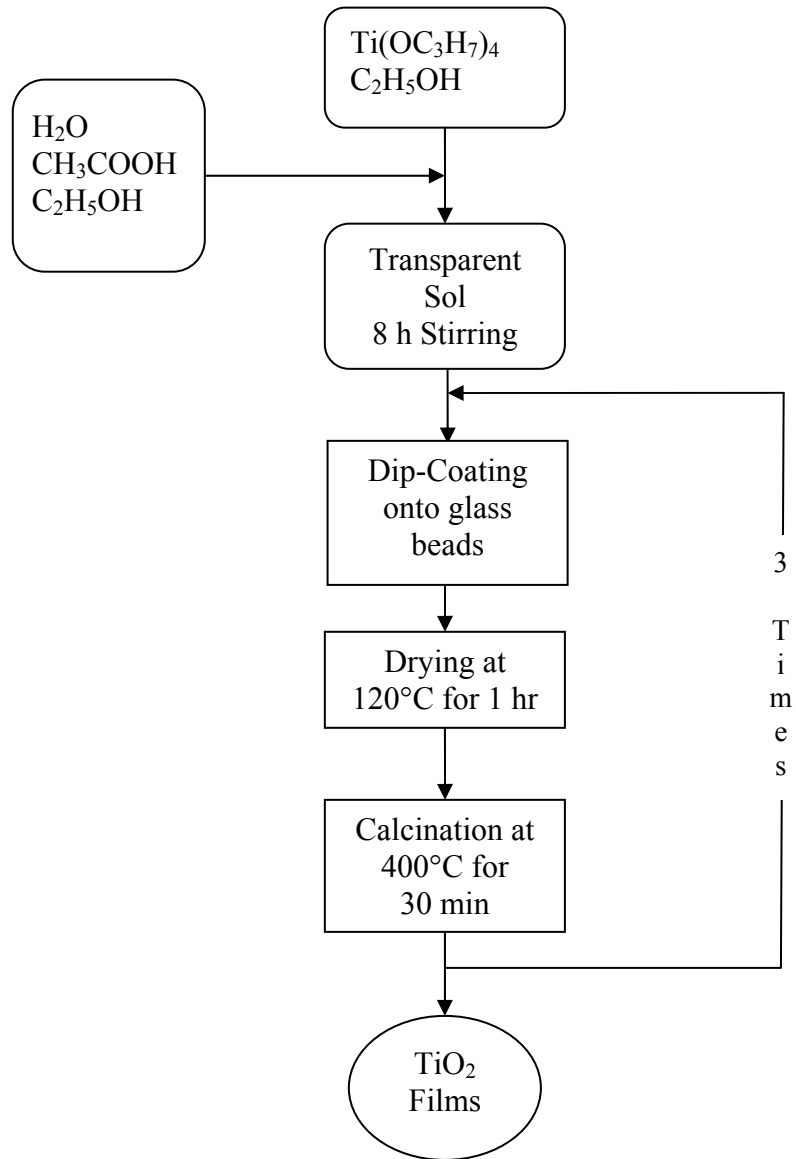


Figure 3.2 Thick film coating procedure

3.2 CATALYST CHARACTERIZATION

The calcination temperatures of the TiO₂ films were determined based on thermo-gravimetric analysis. The analysis was performed on powdered catalysts synthesized using the same sol-gel procedure with V4.1C DuPont 2000 equipment under N₂ flowrate of 75 cc/min and a temperature ramp of 10°C/min between the temperatures 30-900°C.

To determine the average surface area and pore diameter of the TiO₂ catalysts, BET surface areas were measured with TiO₂ powder catalysts synthesized using the same sol-gel procedure. The BET Surface area was measured by automated ASAP 2000 Micromeritics N₂ adsorption equipment.

XRD analysis was done to determine the crystalline phase of the films. The analysis was done using a Philips PW 1840 Diffractometer.

UV-Vis Absorption tests have been performed to make sure that anchoring of light harvesting molecules onto TiO₂ films has been established. Measurements were taken with a Hitachi U 3200 UV-Vis Spectrophotometer, between 300 and 1200 nm, using uncoated beads as reference or blank sample for TiO₂ beads. The absorption spectra of LHM promoted films were measured using TiO₂ coated beads as blank sample.

SEM images have been taken to make sure that coating was established for thin films. The thin films were transparent and they were not visibly detectable. The images were taken with a JSM-6400 Electron Microscope (JEOL). The images are given in Appendix D.

Hydrogen chemisorption measurement was performed with Pt(on)-TiO₂ and Pt(in)-TiO₂ catalysts to enable a comparison between their yields based on the surface Pt atoms. The measurements were done on an adsorption manifold described elsewhere [51]. The chemisorption experiment procedure can be found in a previous M.S. thesis [52].

3.3 CATALYST TESTING

The reaction tests were performed under batch mode in the manifold shown in the Figure 3.3. A picture of the experimental setup can be viewed in Appendix E. The feed side of test setup consists of a CO₂ cylinder and a chamber containing liquid water connected to a main line. The main line enters a glass chamber which was separated from the reaction chamber with a valve. This mid chamber was connected to a vacuum line. A baratron pressure gauge measures the pressure in the chamber. The reaction chamber was put into a wooden box, which has mirror inner walls and was irradiated from one side. Before each reaction run, 16 coated beads are placed into a glass reaction cell, which has a septum for taking gas samples. The beads are then vacuumed for 30 minutes in room temperature to get rid of surface adsorbates. The main line was also vacuumed to empty the gas mixture present in the tubing.

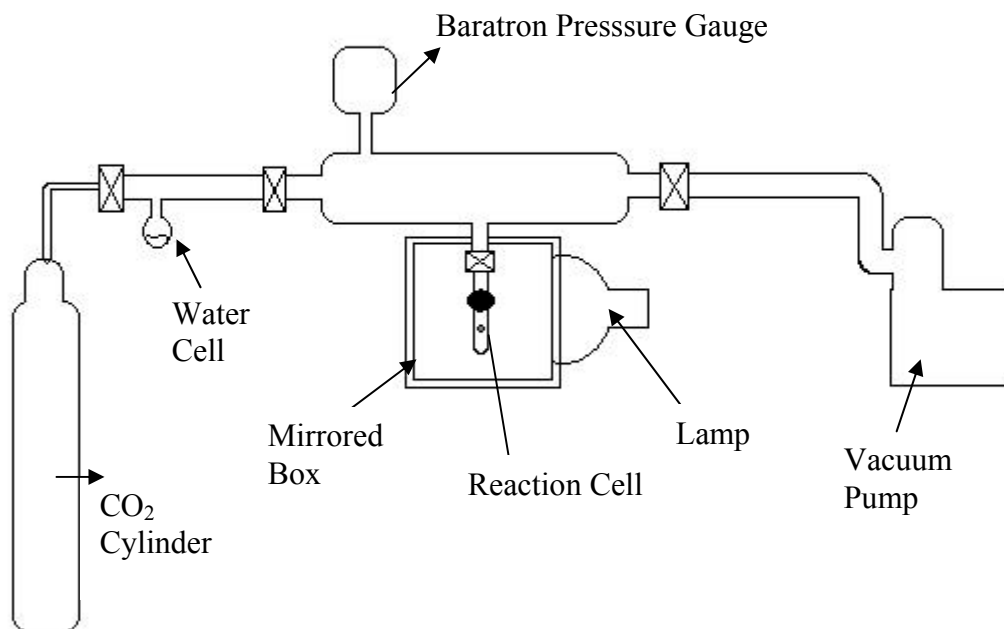


Figure 3.3 Reaction Test Setup

The feed contains ~20 torr of water and ~660 torr of CO₂, which together makes up the atmospheric pressure in Ankara. After vacuuming the chamber water was allowed to evaporate till desired pressure was reached and then CO₂ was fed. The valve between the mid chamber and the reaction cell was then closed and a sample was taken from the cell for 0th minute. The reaction cell was then placed into the wooden box and at last the light was turned on.

The tests were performed under UV and visible light illumination. For UV tests a 150W lamp was used, for visible light tests 75W daylight lamp was used. Measurements were taken at 60th, 120th and 180th minutes of the test run. The products of reaction tests of thin films were analyzed using a HP-4890/A GC equipped with 6' Porapak Q column. For the reaction tests with thick films Varian 3900 GC equipped with Poraplot Q capillary column was used. The settings applied during the experiments are given in Table 3.2.

Table 3.2 GC Operation Parameters

	HP-4890/A	Varian 3900
Column Type	Packed Column 6' Porapak Q	Capillary Column Poraplot Q
Column Flowrate	Column head pressure: 14 psi, when cold	1 cc/min
Injector Temperature	150°C	50°C
Column Temperature	80°C	30°C
Detector Temperature	200°C	220°C

CHAPTER IV

RESULTS and DISCUSSION

4.1 CATALYST CHARACTERIZATION RESULTS

TGA analysis was performed with powdered catalysts to determine the proper calcination procedure for TiO₂ film coating. After the analysis, it was decided that 30 minutes of calcination at 400°C would be enough to evaporate/burn the solvents. The TGA data can be viewed in the Appendix A.

BET Analysis was performed to measure the BET surface area of TiO₂ catalysts. Powdered catalyst prepared using the same sol was used in the BET surface area measurement. Here it was assumed that the coated TiO₂ films have the same surface area as the powdered catalyst. The BET surface area of the catalyst was found to be: 17.9523 m²/g. Average pore diameter was measured as 4.43658 nm.

XRD analysis was done to determine the crystalline phase of the films. Thin films did not show any crystallinity, whereas with thick films some peaks have been observed. The reason that no distinctive peaks have been observable could be that the coating was dilute when compared to the powdered forms.

UV-Vis Absorption tests have been performed to make sure that anchoring of light harvesting molecules onto TiO₂ films has been established. Measurements were done using uncoated beads as reference or blank sample for TiO₂ beads. The characteristic absorption maximum was observed at ~290 nm. The absorption spectra of LHM promoted films were measured using TiO₂ coated beads as blank sample. RuBpy, BrGly and BrAsp containing samples gave absorption peaks at the wavelengths shown in Table 4.1:

Table 4.1 UV-Vis Absorption maxima of RuBpy·TiO₂, BrGly·TiO₂ and BeAsp·TiO₂ Catalysts

Catalyst	Wavelength of absorption maxima (nm)
RuBpy·TiO ₂	380, 480, 590
BrGly·TiO ₂	490, 570, 600, 650
BrAsp·TiO ₂	610, 860

The presence of absorption maxima in the visible range revealed the presence of LHM's on the surface of the three catalysts.

With hydrogen chemisorption measurement the surface Pt atom content of the Pt(on)·TiO₂ catalyst was measured as 0.24 mmolPt/gram catalyst. During the calculations the H/Pt stoichiometry was taken as 1. With the Pt(in)·TiO₂ catalyst the Pt concentration was below the detection limits of the present chemisorption setup.

4.2 REACTION TEST RESULTS

4.2.1 Thin Films

4.2.1.1 UV Light Reaction Tests

Thin film coatings of TiO₂, Pt(in)·TiO₂, Pt(on)·TiO₂, RuBpy·TiO₂ and RuBpy·Pt·TiO₂ catalysts were prepared and tested for carbon dioxide reduction under UV light. The test chamber, as described in detail in Section 2.3, contained ~20 torr water vapor and ~660 torr carbon dioxide as the initial feed. The runs lasted for 3 hours; samples were analyzed with a HP-4890/A GC equipped with 6' Porapak Q column.

The results are reported as micromoles of methane produced per gram catalyst. A packing consists of 16 coated beads. To determine an average weight of

the catalysts, a sample batch was coated using the standard procedure and its weight was used as the gram catalyst per packing value.

4.2.1.1.a) Effect of Platinum addition and Method of Platinum addition on the photocatalytic performance of TiO₂ films

The effect of Pt addition method was investigated by using two different synthesis techniques. As described in detail in Section 2.1.1.2, Pt(in) and Pt(on) catalysts have been prepared by using Pt containing sols and Pt containing aqueous solutions respectively.

The only observable reaction product on TiO₂ and Pt·TiO₂ was methane. Addition of Pt resulted in increase of yields for both synthesis methods. As seen from the Figure 4.1, the photocatalytic activity was in the order of Pt(on)·TiO₂ > Pt(in)·TiO₂ > TiO₂. This increase of photocatalytic activity is explained by decreased electron-hole recombination probability due to the presence of platinum.

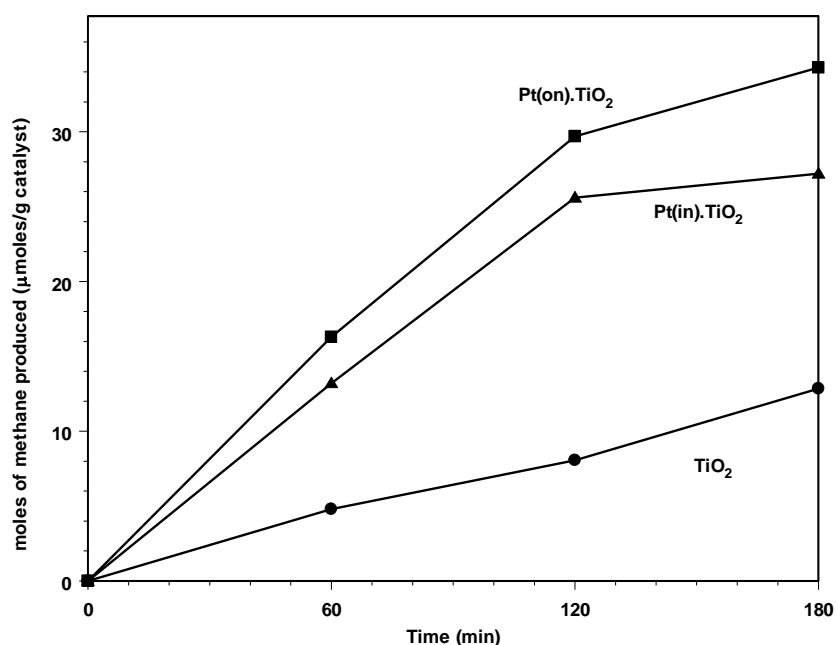


Figure 4.1 Methane yields of TiO₂, Pt(in)·TiO₂ and Pt(on)·TiO₂ thin film catalysts under UV light

For Pt(in) catalyst, H₂ chemisorption measurement could not be performed since the surface Pt amount was below the detection limits. On the other hand, H₂ chemisorption measurements for Pt(on) catalysts yield a surface Pt concentration of 0.24 mmolPt/gram catalyst. This shows that, Pt was partially moved to the bulk of the catalyst for Pt(in) catalyst, which explains the lower yield of Pt(in) catalyst when compared to Pt(on) catalyst.

4.2.1.1.b) Effect of RuBpy addition

Addition of RuBpy onto TiO₂ and Pt(in).TiO₂ catalysts increased the yield of methane formation. Hydrogen evolution was observed however not quantified on RuBpy containing catalyst under UV irradiation. As seen from the Figure 4.2, the order of activity was as follows: RuBpy·Pt(in)·TiO₂ > Pt(in)·TiO₂ > RuBpy·TiO₂ > TiO₂.

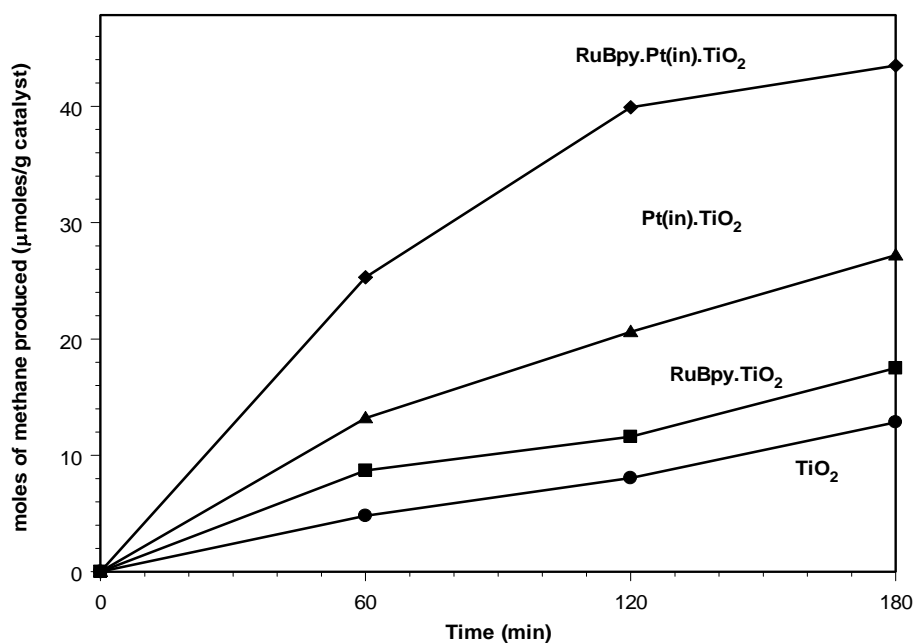


Figure 4.2 Methane yields of TiO₂, Pt(in)·TiO₂, RuBpy·TiO₂ and RuBpy·Pt(in)·TiO₂ thin film catalysts under UV light

The stability of the RuBpy·Pt(in)·TiO₂ catalyst was tested by carrying out the same 3 hour reaction test for 3 consecutive runs, where at the beginning of each run feed conditions were adjusted as the standard conditions.

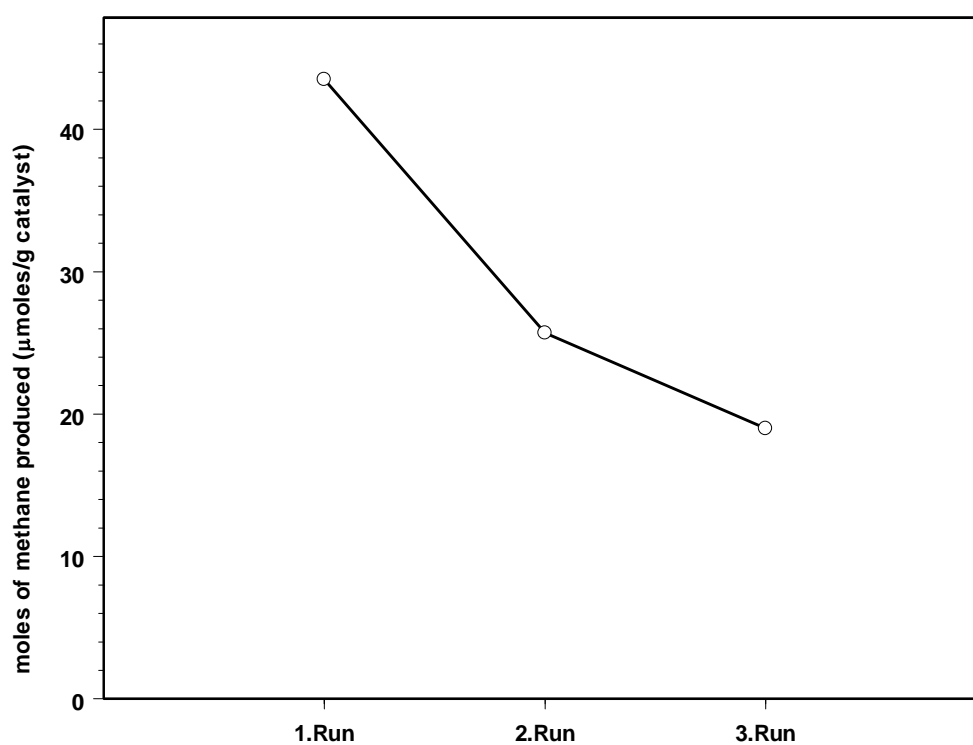


Figure 4.3 Deactivation of RuBpy·Pt(in)·TiO₂ catalyst under UV light during three consecutive test runs

As seen from Figure 4.3, the catalyst was undergoing deactivation. The 3 hour methane yields dropped from 43.5 to 25.7 and 19.0 μmoles/gram catalyst for 2nd and 3rd runs respectively. The deactivation can occur because of decomposition either due to UV irradiation or local high temperatures on the catalyst surface.

4.2.1.2 Visible Light Reaction Tests

RuBpy·Pt(in)·TiO₂, BrGly·Pt(in)·TiO₂ and BrAsp·Pt(in)·TiO₂ catalysts were tested for their photocatalytic carbon dioxide reduction capacities under visible light. To be able to examine the effect of light harvesting molecule addition also TiO₂, Pt(in)·TiO₂ catalysts were tested. The lamp used was a regular 100W daylight lamp. TiO₂, Pt(in)·TiO₂ catalysts did not show any activity under visible light, whereas with all three light harvesting molecules visible light response was observed. This shows that the excited state electrons of LHM's can be transferred to TiO₂, so that they can be used in photocatalytic reactions.

The only detectable reaction product was methane. Methane yields of RuBpy, BrGly and BrAsp promoted Pt(in)·TiO₂ catalysts are given in Figure 4.4.

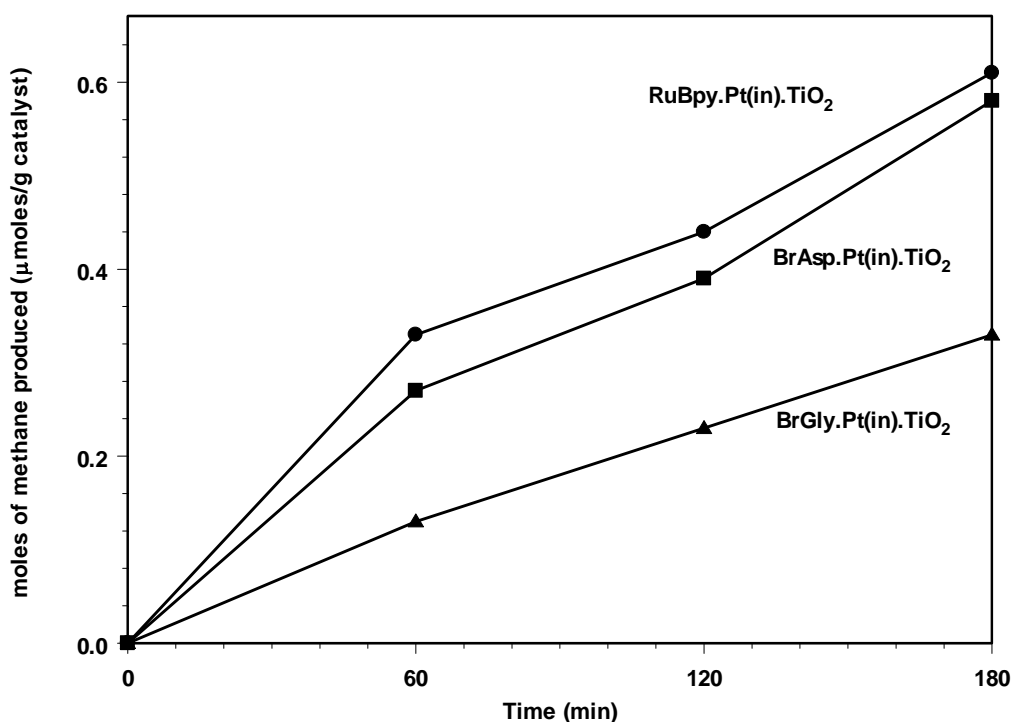


Figure 4.4 Methane yields of RuBpy·Pt(in)·TiO₂, BrGly·Pt(in)·TiO₂ and BrAsp·Pt(in)·TiO₂ thin film catalysts under visible light

4.2.2 Thick Films

TiO₂, Pt(in)·TiO₂, Pt(on)·TiO₂, RuBpy·TiO₂, BrGly·TiO₂, BrAsp·TiO₂, RuBpy·Pt(in)·TiO₂, BrGly·Pt(in)·TiO₂, BrAsp·Pt(in)·TiO₂, RuBpy·Pt(on)·TiO₂, BrGly·Pt(on)·TiO₂ and BrAsp·Pt(on)·TiO₂ thick film catalysts have been prepared and tested for their carbon dioxide reduction capacities under UV and visible light. For the thick films, every catalyst batch consisted of 16 coated beads. The weight of the coating was measured after each step so that the amount of catalyst in each batch was precisely determined.

The chamber used in reaction tests, as described in detail in Section 2.3, contained ~20 torr water vapor and ~660 torr carbon dioxide as the initial feed. The test runs lasted for 3 hours; samples taken from the reaction cell were analyzed with a Varian 3900 GC equipped with Poraplot Q capillary column.

4.2.2.1 UV Light Reaction Tests

4.2.2.1.a) Effect of Platinum addition and Method of Platinum addition on the photocatalytic performance of TiO₂ films

Pt(in)·TiO₂ and Pt(on)·TiO₂ catalysts were prepared and tested to examine the effect of platinum addition procedure on the photocatalytic activity of TiO₂ thin films. As in the case of thin films the only detectible reaction product was methane. Additionally, the effect of Pt addition procedure was similar to the results of thin film tests. As seen from Figure 4.5, Pt(on) catalysts prepared using aqueous solution of Pt salt showed higher activity than the Pt(in) catalysts prepared using a Pt containing sol. The increase in the yields when compared to plain TiO₂ films was due to the fact that the presence of Pt atoms results in charge separation on the catalyst surface. This lowers the probability of decay of the excited state by charge recombination. On the other hand, Pt(in) catalysts showed lower yields than Pt(in) catalysts, which can be explained by the low surface concentration of Pt. If Pt was

shifted to the bulk of the TiO_2 film, since it can not act as a reaction site, it will not serve as a charge separator and will be useless for the photocatalytic reactions. Moreover, when Pt was in the bulk, the band gap of the TiO_2 will inevitably be modified altering the bulk states. In addition, the surface state modifications can also be expected.

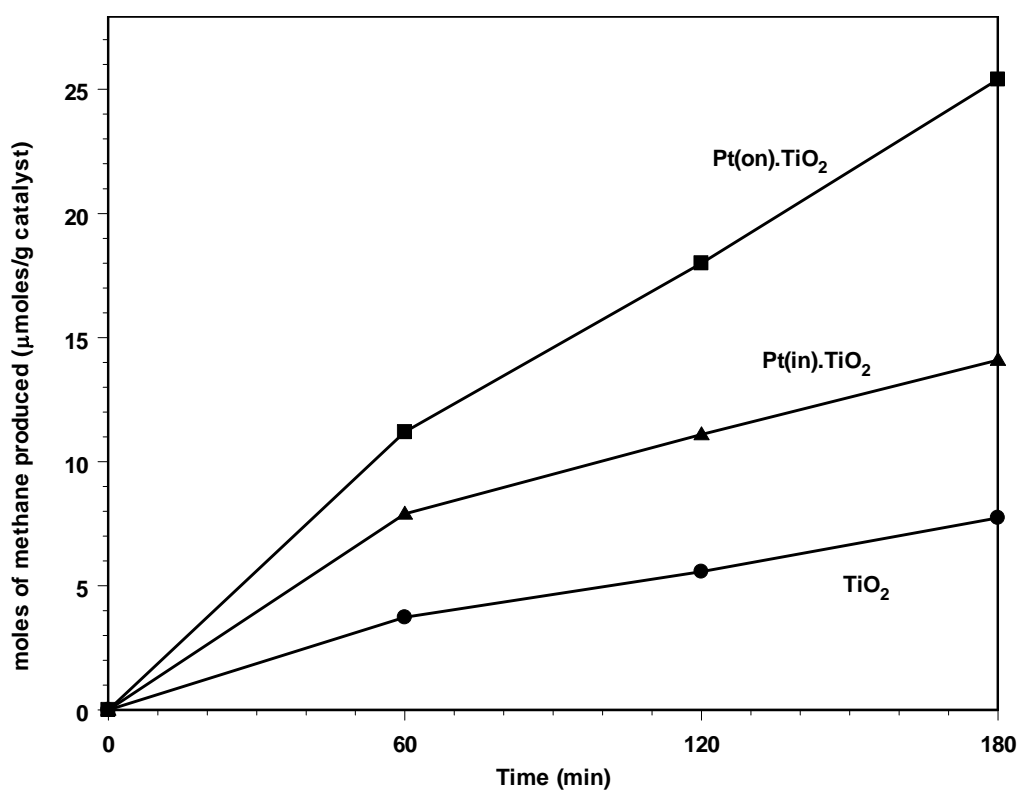


Figure 4.5 Methane yields of TiO_2 , $\text{Pt(in)}\cdot\text{TiO}_2$ and $\text{Pt(on)}\cdot\text{TiO}_2$ thick film catalysts under UV light

4.2.2.1.b) Effect of LHM addition on the photocatalytic activity of TiO₂ thick films

RuBpy·TiO₂, BrGly·TiO₂ and BrAsp·TiO₂ catalysts were prepared and tested to see the effect of LHM promotion on the photocatalytic activity of plain TiO₂ films. As seen from Figure 4.6, LHM addition onto TiO₂ films resulted in a drastic decrease of methane yields. RuBpy and BrAsp containing catalysts gave similar 3 hour yields where as BrGly containing films had a lower activity.

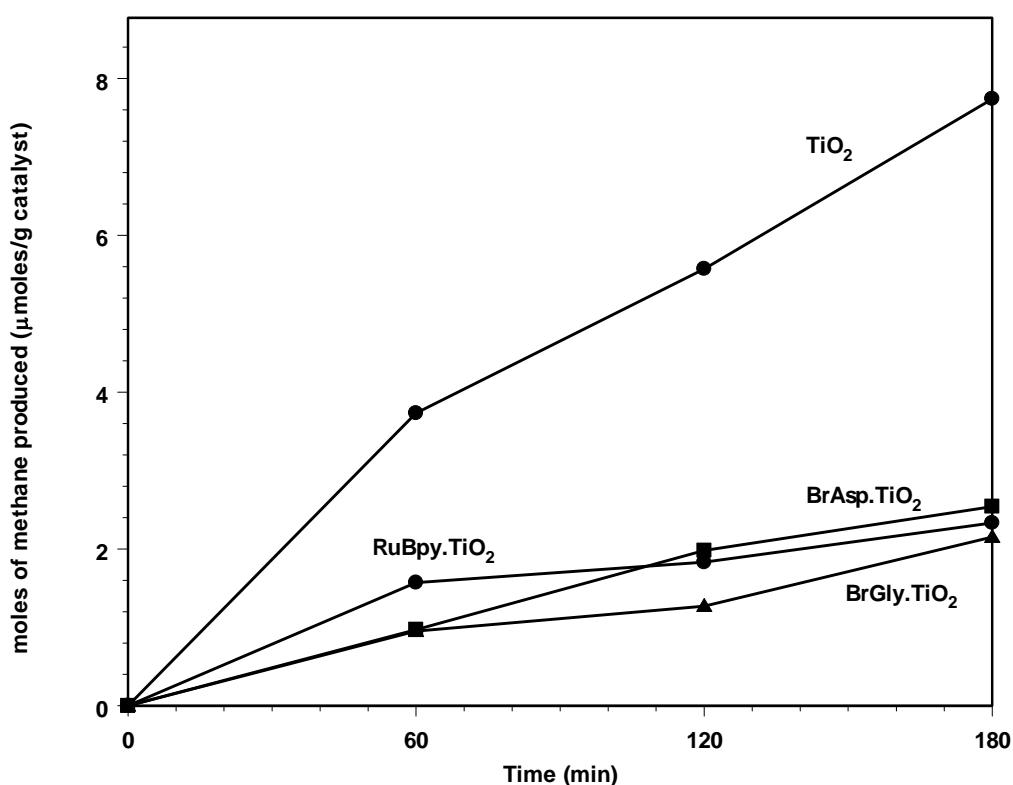


Figure 4.6 Methane yields of RuBpy·TiO₂, BrGly·TiO₂, BrAsp·TiO₂ and TiO₂ film catalysts under UV light

The decrease in yields of methane with LHM containing catalysts can be either due to the different mechanisms of relaxation of excited states in the presence

of LHM's, or due to the filtering effect of those organic molecules for UV light. Since those absorption bands of those molecules are in the visible range, those molecules are not expected to participate in excitation processes in UV light. They could only serve to charge separation, however in thick film experiments the results indicated that they did not contribute to the photocatalytic activity of TiO₂ thick films.

4.2.2.1.c) Effect of LHM addition on the photocatalytic activity of Pt·TiO₂ thick films

Thick films of RuBpy·Pt(in)·TiO₂, BrGly·Pt(in)·TiO₂, BrAsp·Pt(in)·TiO₂, RuBpy·Pt(on)·TiO₂, BrGly·Pt(on)·TiO₂ and BrAsp·Pt(on)·TiO₂ have been prepared and tested for their carbon dioxide reduction capacities under UV light.

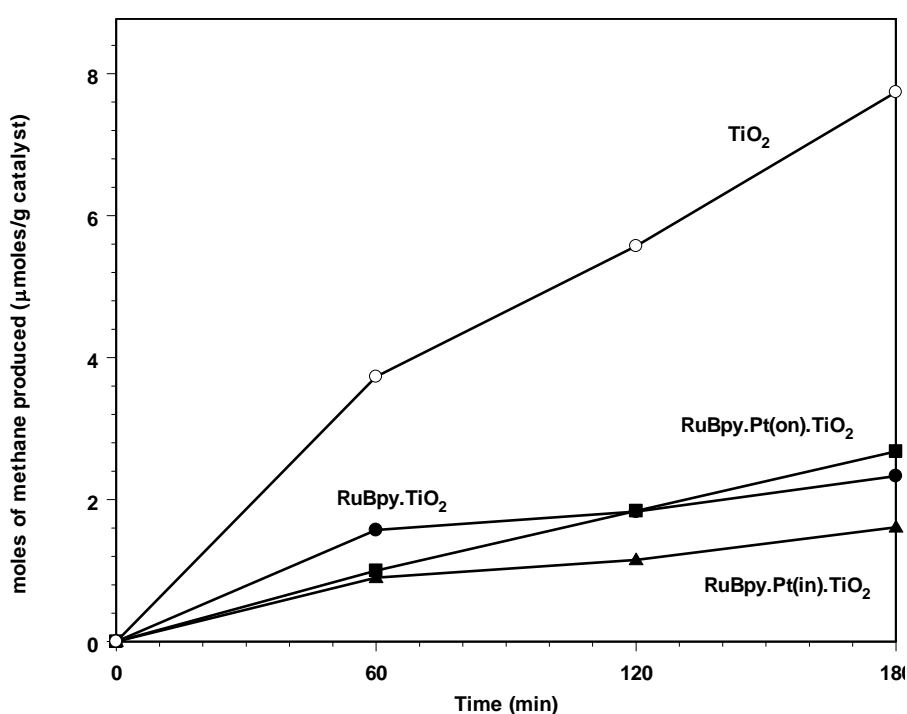


Figure 4.7 Methane yields of TiO₂, RuBpy·TiO₂, RuBpy·Pt(in)·TiO₂ and RuBpy·Pt(on)·TiO₂ thick film catalysts under UV light

As seen from the Figure 4.7, addition of RuBpy on Pt(in)·TiO₂ and Pt(on)·TiO₂ thick film catalysts resulted in lower yields than plain TiO₂ films under UV light. As observed previously with Pt(in)·TiO₂ and Pt(on)·TiO₂ catalysts without RuBpy, addition via aqueous solution resulted in a higher activity.

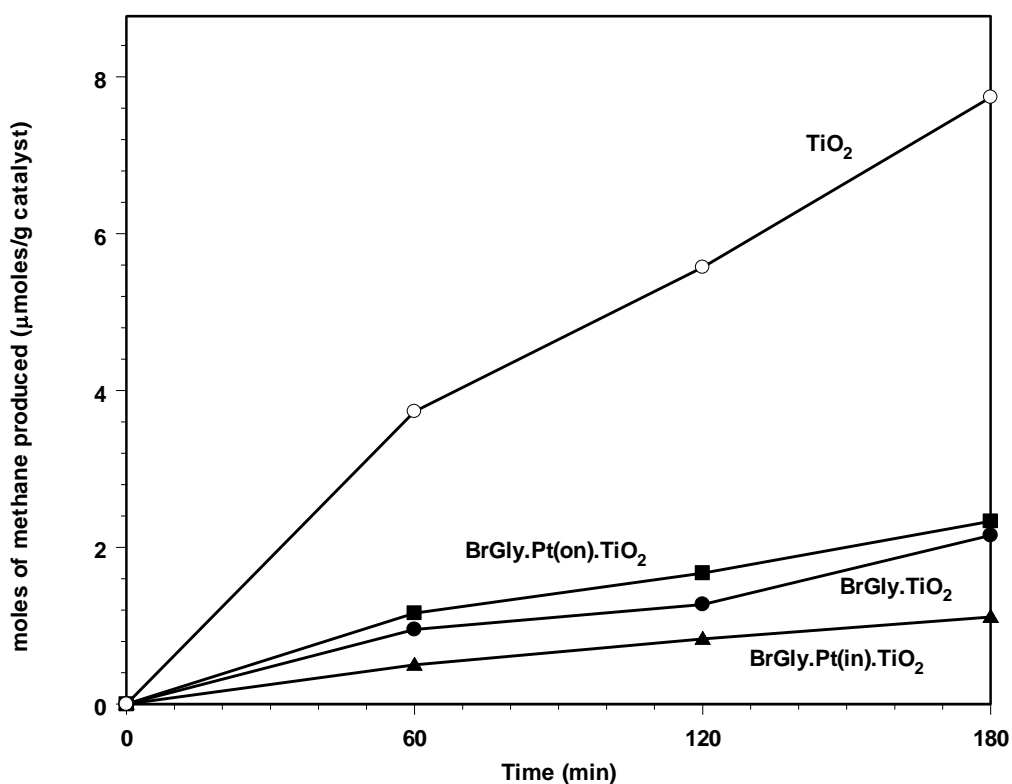


Figure 4.8 Methane yields of TiO₂, BrGly·TiO₂, BrGly·Pt(in)·TiO₂ and BrGly·Pt(on)·TiO₂ thick film catalysts under UV light

As seen from Figure 4.8 and 4.9, addition of BrGly and BrAsp onto Pt(in) and Pt(on) thick film catalyst resulted in a decrease of photocatalytic performance when compared with the plain TiO₂ thick films. As in the case of RuBpy containing Pt(in)·TiO₂ and Pt(on)·TiO₂ films, addition of Pt via aqueous solution resulted in a catalyst with higher activity for both BrGly and BrAsp containing catalysts.

When BrGly and BrAsp were compared for their photocatalytic activities; for both Pt·TiO₂ and TiO₂ supported catalysts BrAsp containing catalysts showed higher activity. The higher activity of BrAsp could be due to its double carboxylic ends, which may result in a better anchoring onto the support surface.

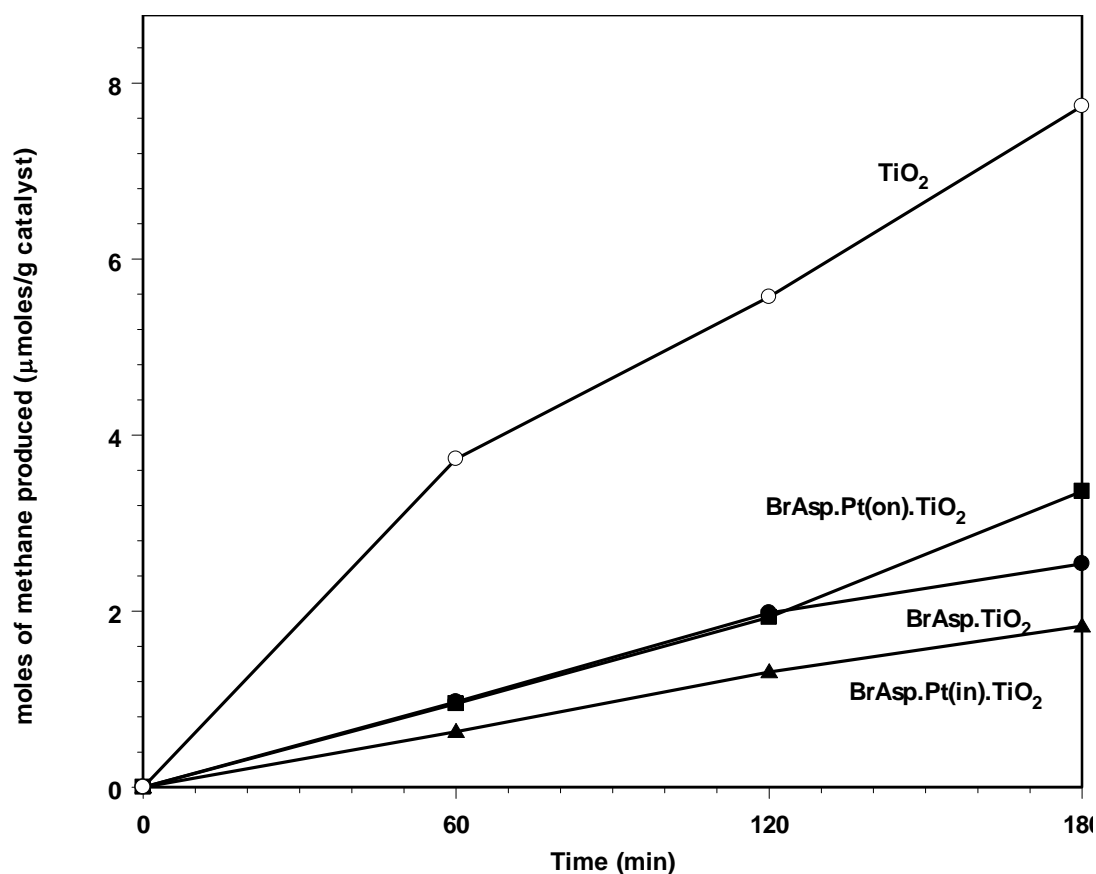


Figure 4.9 Methane yields of TiO₂, BrAsp·TiO₂, BrAsp·Pt(in)·TiO₂ and BrAsp·Pt(on)·TiO₂ thick film catalysts under UV light

4.2.2.2 Visible Light Reaction Tests

TiO₂, Pt(in)·TiO₂, Pt(on)·TiO₂, RuBpy·TiO₂, BrGly·TiO₂, BrAsp·TiO₂, RuBpy·Pt(in)·TiO₂, BrGly·Pt(in)·TiO₂, BrAsp·Pt(in)·TiO₂, RuBpy·Pt(on)·TiO₂,

BrGly·Pt(on)·TiO₂ and BrAsp·Pt(on)·TiO₂ thick film catalysts have been prepared and tested for their photocatalytic carbon dioxide reduction performances under visible light.

TiO₂ and Pt·TiO₂ catalysts did not show any photocatalytic activity under visible light. Addition of all LHM's onto TiO₂ and Pt·TiO₂ films resulted in visible light active catalysts.

4.2.2.2.a) Effect of LHM addition on the photocatalytic activity of TiO₂ thick films

The aim of synthesizing LHM promoted TiO₂ films was to combine the visible light excitation potential of the organic dyes and catalytic performance of TiO₂ for carbon dioxide reduction. The excited state electrons on the dye molecule can be injected to the TiO₂ structure as it was in the working principle of dye synthesized solar cells [2.42], which result in photocatalytic activity in the visible region.

The three hour reaction tests of RuBpy·TiO₂, BrGly·TiO₂ and BrAsp·TiO₂ thick film catalysts showed that the excitation-injection mechanism was working successfully. As seen from the Figure 4.10, methane production was observed, the activities were in the order of BrAsp·TiO₂ > RuBpy·TiO₂ > BrGly·TiO₂.

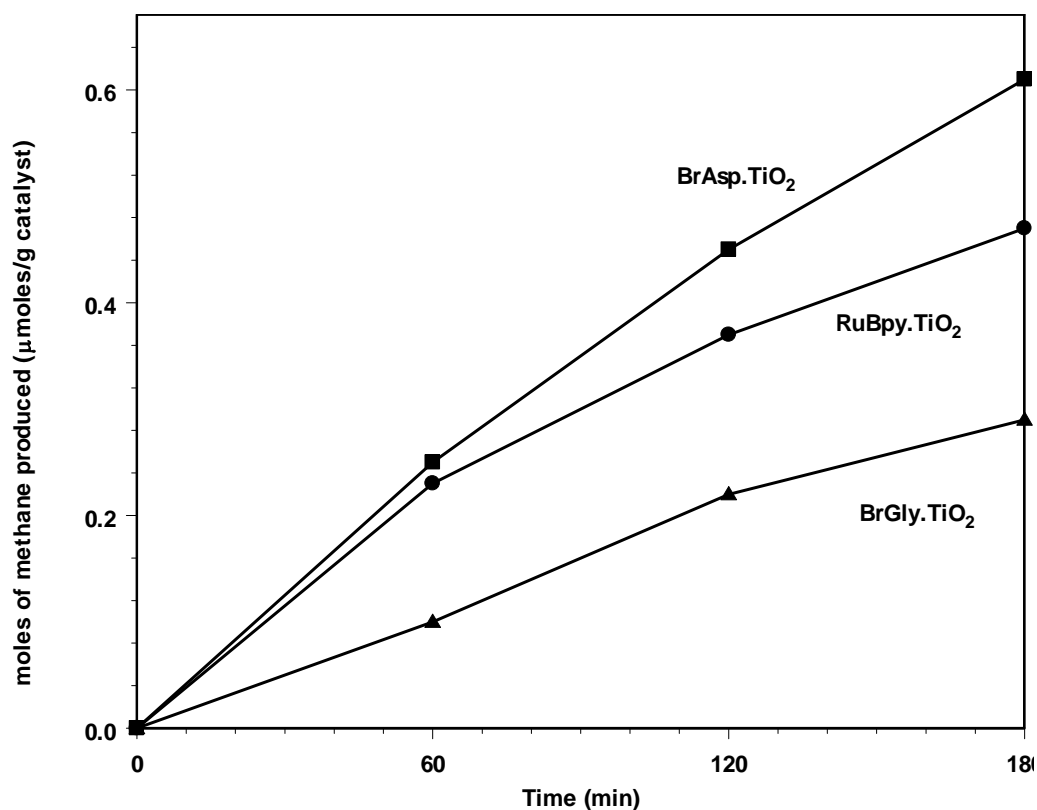


Figure 4.10 Methane yields of RuBpy·TiO₂, BrGly·TiO₂ and BrAsp·TiO₂ thick film catalysts under visible light

4.2.2.2.b) Effect of LHM addition on the photocatalytic activity of Pt·TiO₂ thick films

RuBpy, BrGly and BrAsp promoted Pt(in) and Pt(on) catalysts were synthesized and tested for their carbon dioxide reduction performances under visible light. As seen from Figure 4.11-4.13, all three catalysts showed photocatalytic activity in the visible region. Addition of Pt via aqueous solution resulted in the catalysts with highest methane yields.

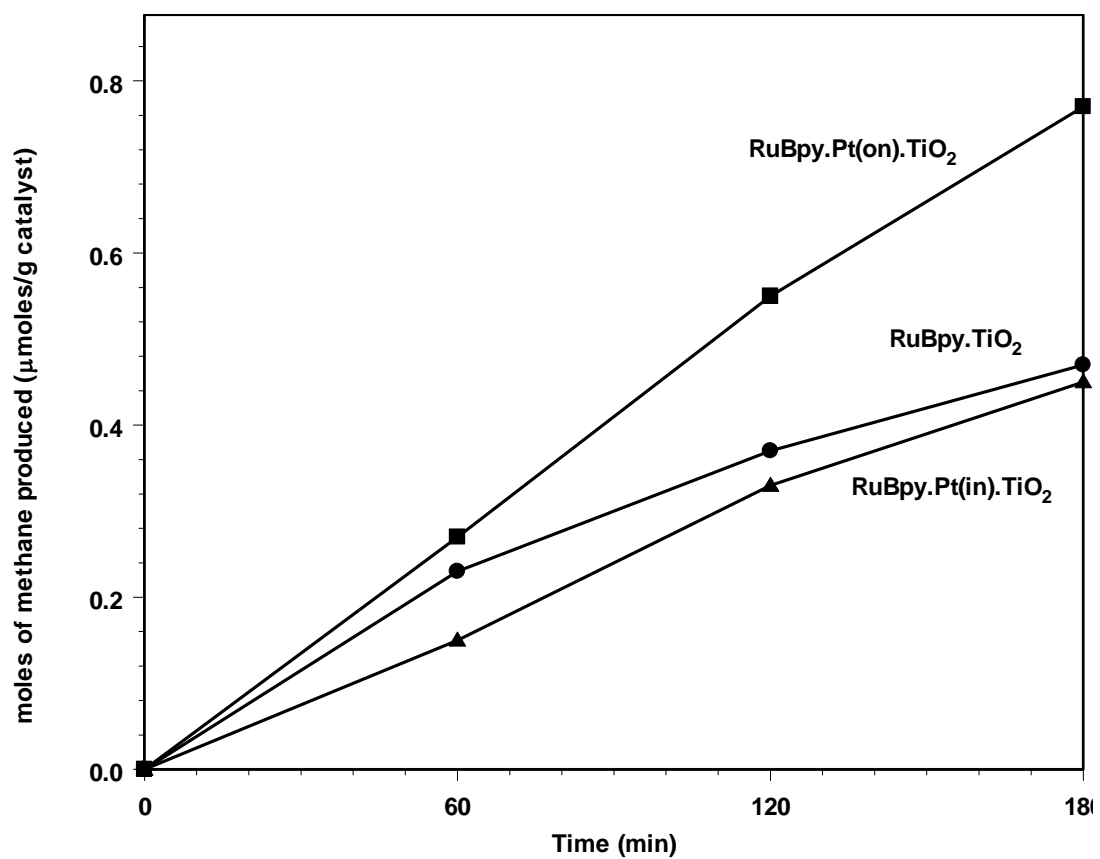


Figure 4.11 Methane yields of RuBpy·TiO₂, RuBpy·Pt(in)·TiO₂ and RuBpy·Pt(on)·TiO₂ thick film catalysts under visible light

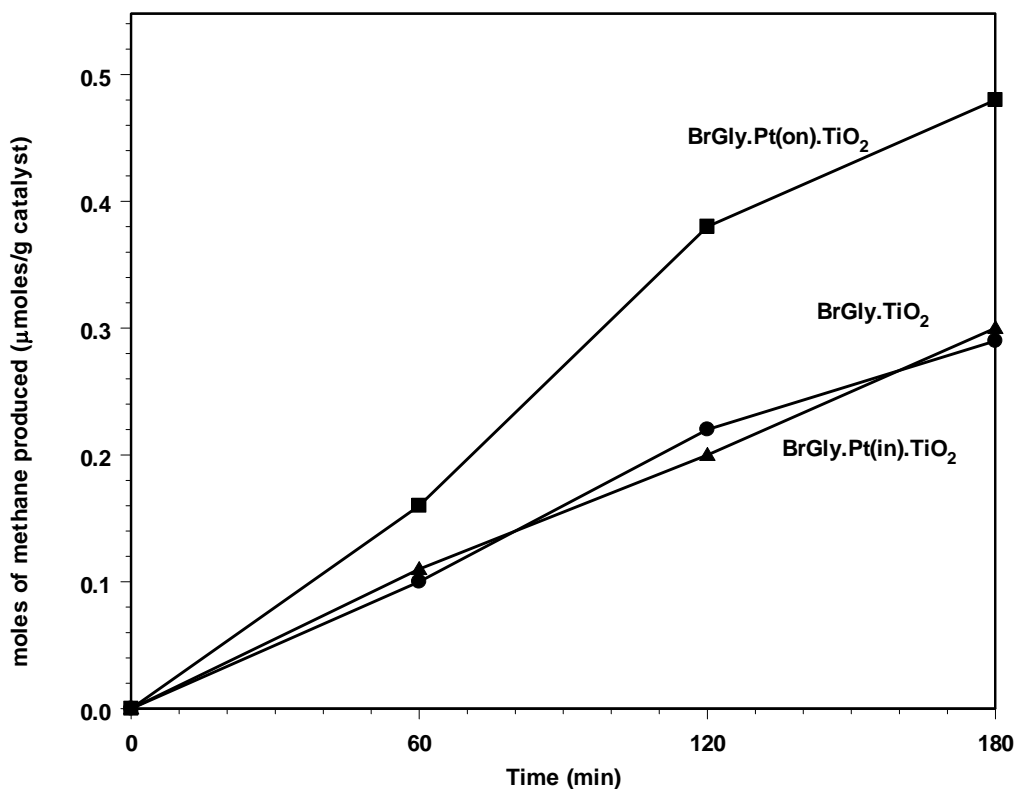


Figure 4.12 Methane yields of BrGly·TiO₂, BrGly·Pt(in)·TiO₂ and BrGly·Pt(on)·TiO₂ thick film catalysts under visible light

As seen from the Figures 4.11-4.13, addition of Pt via Pt containing sol resulted in either no significant change or even decrease in photocatalytic activity. The presence of Pt in the bulk of TiO₂, as previously explained, may increase the probability for electron-hole recombination. It may also modify the band gap of TiO₂, effecting the surface and bulk oxidation states.

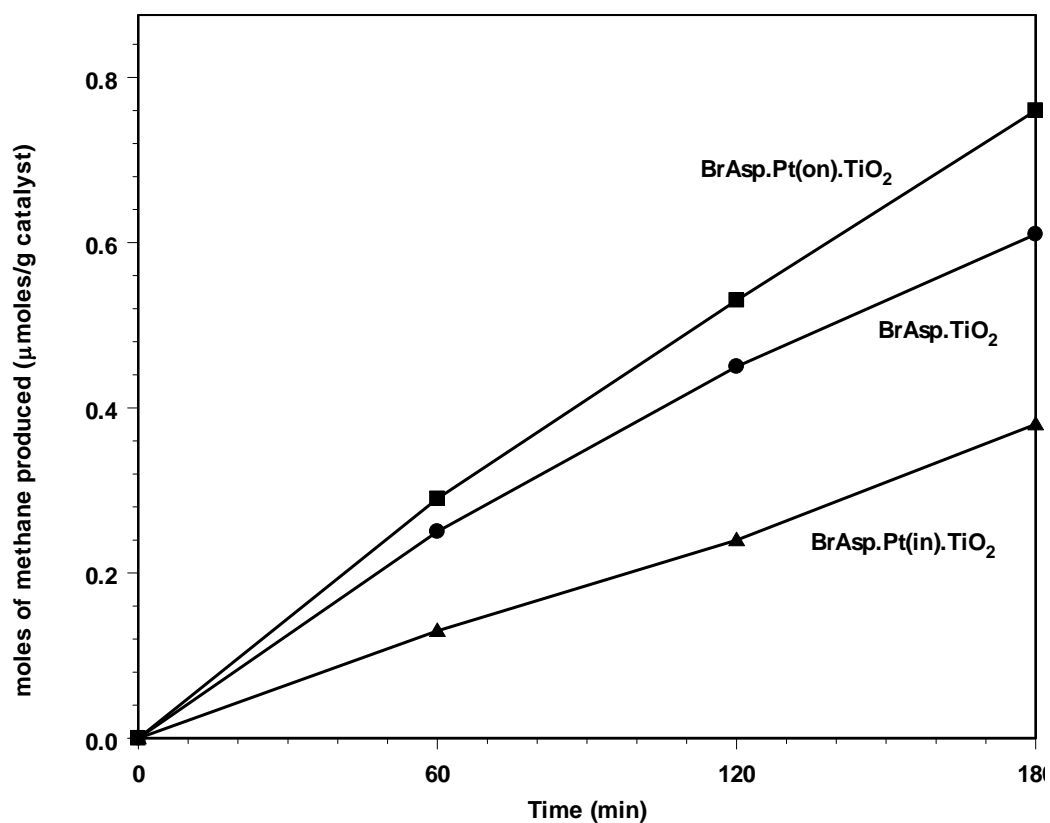


Figure 4.13 Methane yields of BrAsp·TiO₂, BrAsp·Pt(in)·TiO₂ and BrAsp·Pt(on)·TiO₂ thick film catalysts under visible light

The LHM promoted films showed highest methane yields with the recipe LHM.Pt(on).TiO₂. As seen from the Figure 4.14, when the photocatalytic activity of the three LHM's was compared it was in the order of: RuBpy·Pt(on)·TiO₂ ~ BrAsp·Pt(on)·TiO₂ > BrGly·Pt(on)·TiO₂.

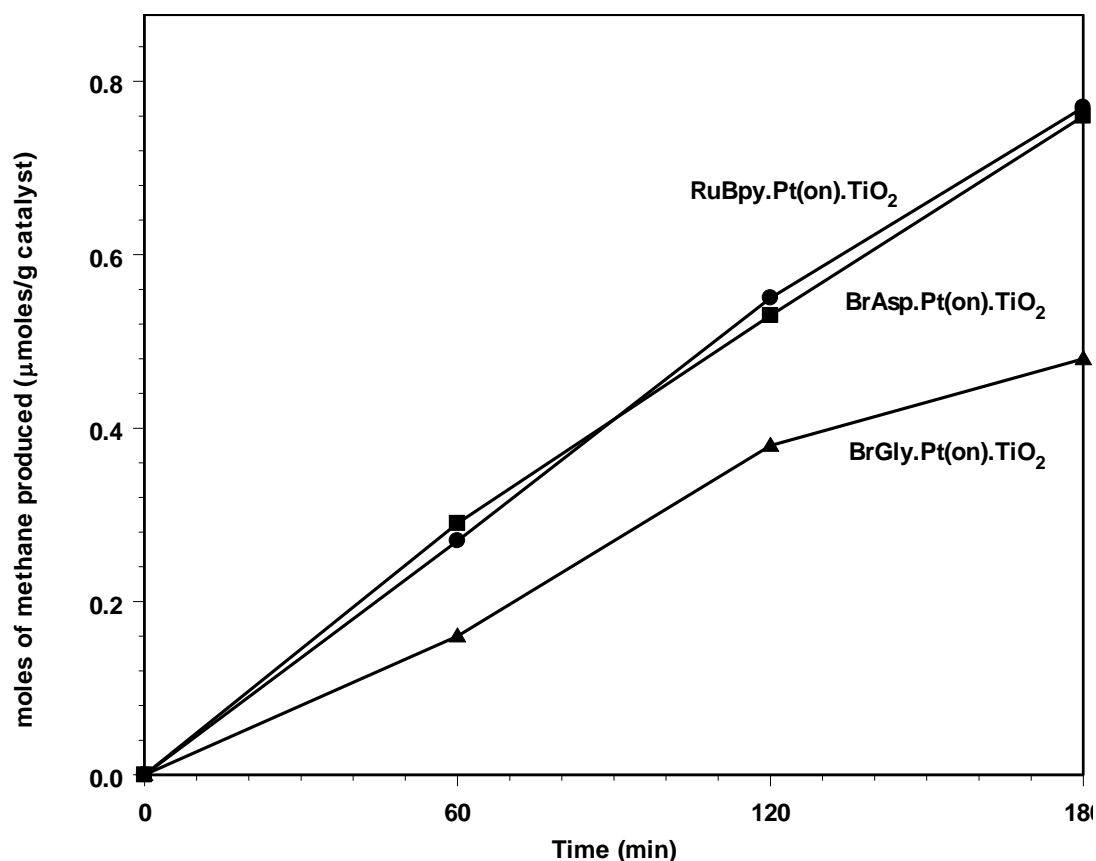


Figure 4.14 Methane yields of RuBpy·Pt(on)·TiO₂, BrGly·Pt(on)·TiO₂ and BrAsp·Pt(on)·TiO₂ thin film catalysts under visible light

As a result, visible light activation of TiO₂ based catalysts was established via addition of organic dye molecules onto the surface. Besides the commercially available RuBpy also novel materials synthesized at METU were successfully anchored to TiO₂ surface during this study. Besides the successfully proven photo-therapeutic applications, BrGly and especially BrAsp molecules showed promising performance for photocatalytic applications.

4.2.3 Thin Films vs. Thick Films

For the scope of this study, both thin and thick films were synthesized and tested for their photocatalytic carbon dioxide reduction performances. The thin films synthesized in this project were transparent where as the thick films were nearly opaque. Therefore it was expected that the thin films with low bulk TiO₂ content will give higher yields for both UV and visible light experiments when compared to the thick TiO₂ films. The Figure 4.15 and 4.16 shows clearly that the thin films had a higher photocatalytic activity under UV and visible light.

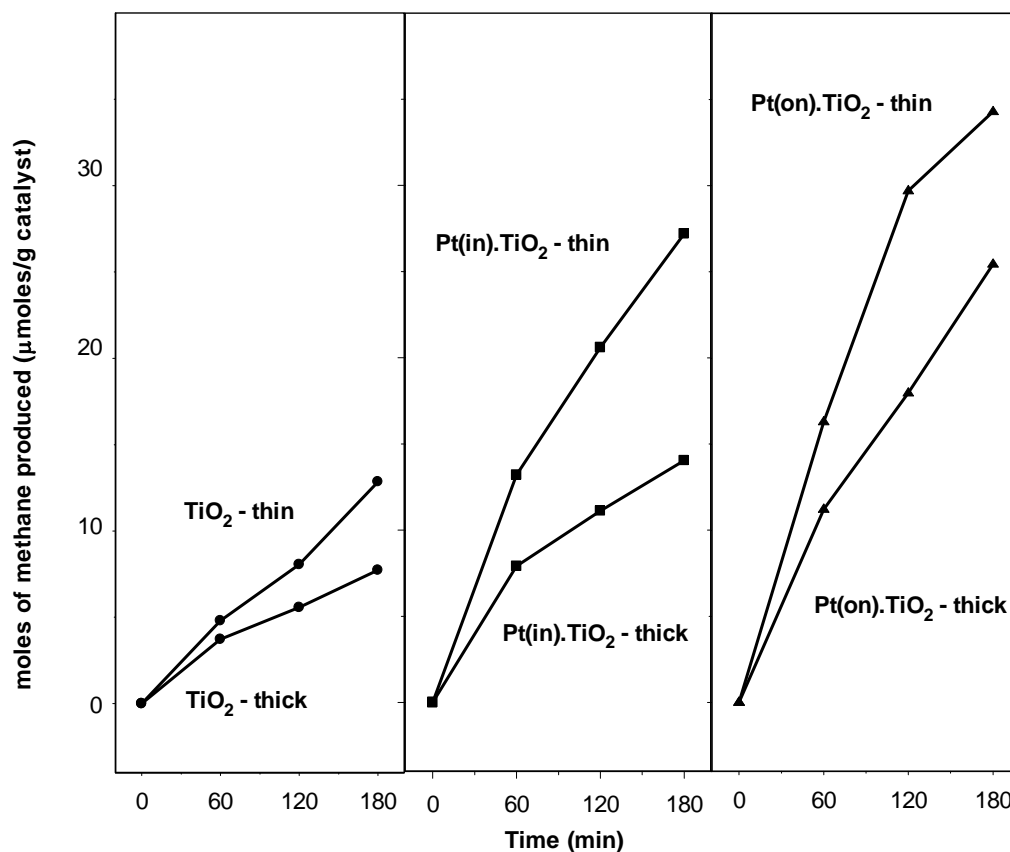


Figure 4.15 Comparison of methane yields of thick and thin films under UV light

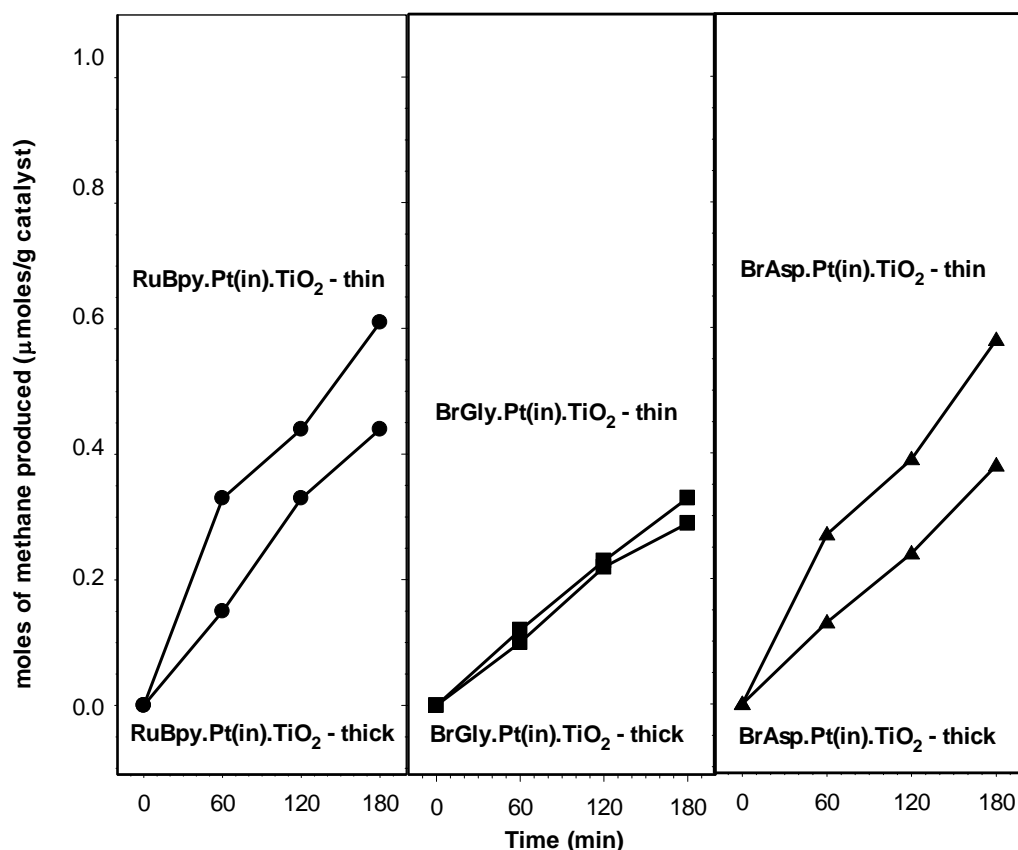


Figure 4.16 Comparison of methane yields of thick and thin films of LHM.Pt(in).TiO₂ catalysts under visible light

Throughout the study thin films have performed better than the thick films of same type. However with the RuBpy·Pt(in)·TiO₂ thin films under UV light a much more significant change was observed. RuBpy addition resulted in decrease of the yields for thick films where as the trend was the opposite with the thin films. The highest yield in this study was observed with RuBpy·Pt(in)·TiO₂ thin films.

Another comparison between thick and thin films could be made based on the yields per coated bead. In Figure 4.17, methane yields per bead are shown for thick and thin film catalysts.

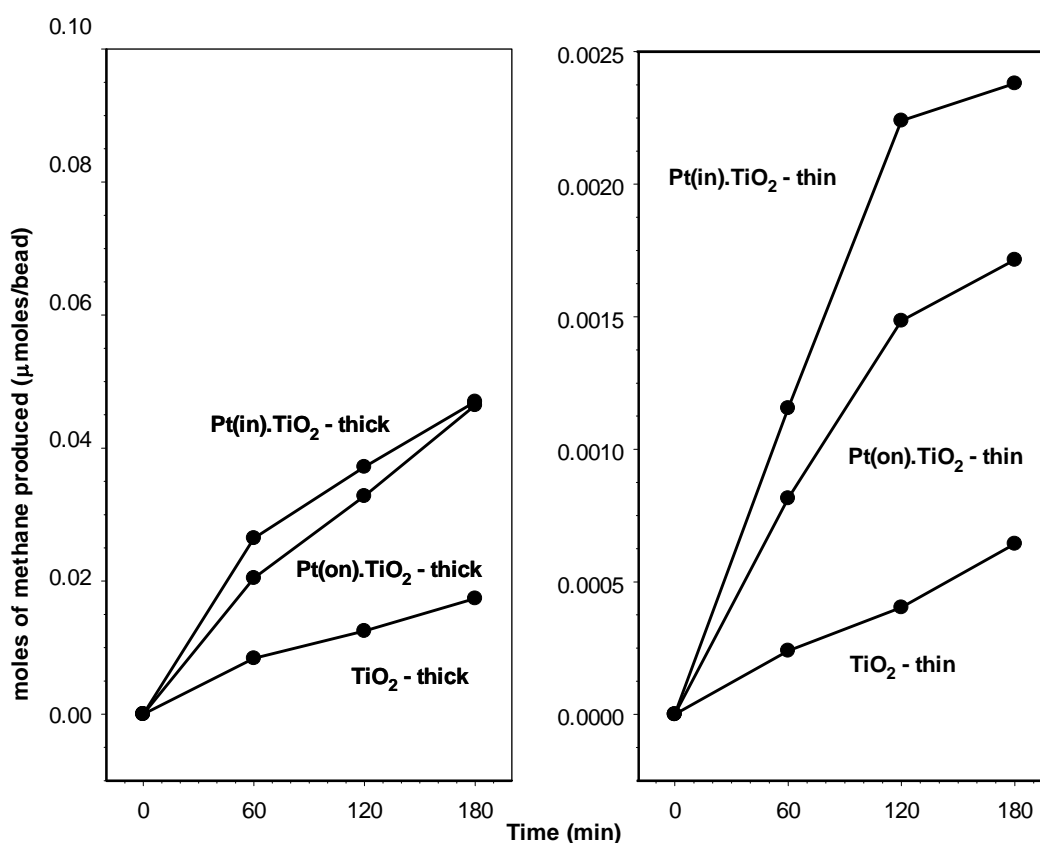


Figure 4.17 Comparison of methane yields per coated bead of thick and thin films under UV light

When UV light performances of thin and thick TiO₂, Pt(in)·TiO₂ and Pt(on)·TiO₂ are compared it was seen that for thick films the yield per bead value was not significantly changing with Pt addition method. For the thin films the difference was greater and Pt(in) catalysts gave higher yield per bead. This was due to the higher amount of photocatalytic material coated onto the bead surface.

As a result, it was observed that on a weight basis thin film catalysts have shown higher photocatalytic activity than the thick films. However, on a bead based comparison the TiO₂, in yield was higher than an order of magnitude. Therefore, the scaling up by thicker coating was found to be promising.

CHAPTER V

CONCLUSIONS

The aim of this study was to test the limits of photocatalytic reduction of CO₂ over Pt and light harvesting dye promoted TiO₂ thin films under UV and visible light. TiO₂ thin film catalysts are coated onto 1 cm long hollow glass beads via a common sol-gel procedure and dip coating technique. TiO₂ thin films were promoted by Pt and three different light harvesting molecules; RuBpy, BrGly and BrAsp. Their SEM, XRD, UV-Vis spectroscopy and hydrogen chemisorption characterizations are performed. The presence of visible light absorption peaks in the UV-Vis spectra revealed the presence of light harvesting molecules on the surface of the synthesized films.

The main reaction product was methane. With RuBpy containing catalyst under UV light, hydrogen production was observed but could not be quantified. The results indicated that Pt addition resulted in higher methane yields in UV experiments. Addition procedure of Pt to TiO₂ played an important role in the photocatalytic activity. Catalysts showed higher activity when Pt was added after the TiO₂ coating via an aqueous solution containing Pt. The yields were lower for the catalysts which have been coated with a Ti and Pt containing sol. For the former case Pt clusters were at the surface where they could promote the surface activity, which was also shown with hydrogen chemisorption experiments. For the latter case, monodispersed Pt atoms stayed in the bulk and showed a lower activity.

Use of dyes with visible range absorption bands as promoters made electron excitation under visible light possible. This resulted in photocatalytic activity under visible light, which was not observed with unpromoted and Pt promoted TiO₂ thin film catalysts. As in the case of UV-light experiments, Pt addition procedure played

an important role in the photocatalytic activity of light harvesting molecule added films. The only quantifiable reaction product was methane. Production of CO was also observed but could not be quantified. The activities of the light harvesting molecule containing catalysts was in the order of RuBpy ~ BrAsp > BrGly.

For the thick films, light harvesting molecule addition resulted in no change or if any in a decrease for UV light experiments. This was explained with the filtering property of those dyes for UV light. Also the excited electrons of TiO₂ are transferred to the light harvesting molecules where they relax via non-reactive pathways.

The comparison between thick and thin films showed that the thin films have higher photocatalytic activity than the thick films. However, since the coating per bead value was too low with thin films their overall yields and yield per bead values are more than an order of magnitude lower than thick films. Therefore, the scaling up of the system by thicker coating was found to be successful.

As a result, visible light activation of TiO₂ films was successfully realized, by light harvesting molecule promotion. Also it was shown that Pt addition has a positive effect on photocatalytic activity of TiO₂ films, which was in good agreement with the studies in the literature.

CHAPTER VI

RECOMMENDATIONS

This study has shown that visible light activation of TiO₂ can be realized by light harvesting molecule promotion. It was also observed that Pt addition has a positive effect on the photocatalytic activity. Moreover the effect of Pt addition procedure also played a role in the photocatalytic properties of the synthesized catalysts.

At this stage, a detailed characterization of the catalysts is needed to obtain more quantitative results. The yields in this study are based on the catalyst weight. However the amount of promoter loading could not be determined. Therefore the reason of the greater activity of BrAsp than BrGly is not clear. It may be due to the higher photoresponse of BrAsp. It may also be observed because of the high surface binding capacity of the BrAsp. The surface loading of the dyes have to be measured for a better quantification. Moreover, dye loading has to be done using dye solutions with different concentrations and their UV-Vis spectras and their reaction test results will help in understanding the effect of dye loading.

The thicknesses of the films have to be measured. For a detailed study more than two concentrations of the coating Sol can be prepared and the effect of Sol concentration on film thickness can be examined.

The H₂O/CO₂ ratio in the reaction cell is restricted by the vapor-pressure of water at the room temperature, since water feeding is done via evaporation. To be able to try higher H₂O/CO₂ ratios, the setup can be heated to higher temperatures.

The addition of Pt resulted in an increase for both synthesis methods, Pt(in) and Pt(on). It is claimed that Pt addition results in charge separation and thereby increases the yields. However it is also known that Pt plays an important role in hydrogen chemistry. The higher activity of Pt containing catalysts may also come

from the chemical activity of Pt not the electrochemical activity. Therefore light responses of the molecules and these reactions have to be modeled on atomic scale.

Methanol production could not be detected with present equipment in the lab. Moreover, with some of the catalysts hydrogen and carbon monoxide production was observed but not quantified. These quantifications have to be done. The reaction mechanism till methane can go through methane or carbon monoxide production steps. At the moment, due to lack of sensitive equipment no conclusions could be reached about the reaction mechanism. It will be only possible when in operando monitoring of the catalyst could be done via FTIR.

REFERENCES

- [1] Jaros, M., *Physics and Applications of Semiconductor Microstructures*, Clarendon Press, New York (1989)
- [2] Graetzel, M., *Nature*, 414, 338-344 (2001)
- [3] Julliard, M., and Chanon, M., *Chem. Rev.*, 83, 425-506 (1983)
- [4] Abe, T., Kaneko, M., *Prog. Polym. Sci.*, 28, 1441-1488 (2003)
- [5] Anpo, M., Tundo, P., Anastas, P., (Eds.), *Green Chemistry*, Oxford University Press, Oxford (2000)
- [6] a) Serhan Özbek, *Studies on Photocatalytic Reactions: Heterogeneous Photocatalysis by Titanium dioxide*, Master's Thesis, Chemical Engineering Department, METU, Ankara (1998)
- b) Ozbek, S., and Uner, D.O., "The deactivation behaviour of the TiO₂ used as photocatalyst for benzene oxidation", *Stud. Surf. Sci. Catal. (Catalyst deactivation)* 126, Netherlands, 411-414 (1999)
- [7] a) İstem Özen, *Thermal and Photocatalytic Oxidation of Carbon monoxide over Titanium dioxide – Effects of Platinum Deposition*, Master's Thesis Chemical Engineering Department, Ankara, METU (2001)
- b) Ozen, I., and Uner, D., "Heterogeneous photo and thermal catalytic oxidation of CO: effects of metal deposition", *Stud. Surf. Sci. Catal. (Reaction Kinetics and the development and operation of catalytic processes)* 133, Netherlands, 445-452 (2001)
- [8] Matsuoka, M., Anpo, M., *J. Photochem. Photobiol. C: Photochem.Rev.*, 3, 225–252 (2002)

- [9] Anpo, M., Takeuchi, M., *J. Catal.*, 216, 505–516 (2003)
- [10] Linsebigler, A. L., Lu, G., Yates, J. T., *Chem. Rev.*, 95, 735-758 (1995)
- [11] Gelover, S., Mondragón, P., Jiménez, A., *J. Photochem. Photobiol. A: Chemistry*, 165, 241–246 (2004)
- [12] Ohno, T., Tanigawa, F., Fujihara, K., Izumi, S., Matsumura, M., *J. Photochem. Photobiol. A:Chemistry*, 127, 107-110 (1999)
- [13] Sayama, K., Mukasa, K., Abe, R., Abe, Y., Arakawa, H., *J. Photochem. Photobiol. A:Chemistry*, 148, 71-77 (2002)
- [14] Nguyen, T.-V., Kim, S., Yang, O-B., *Catal. Commun.*, 5, 59–62 (2004)
- [15] Inoue, T., Fujishima, A., Konishi, S., Honda, K., *Nature*, 277, 637 (1979)
- [16] Anpo, M., Yamashita, H., Ikeue, K., Fujii, Y., Zhang, S.G., Ichihashi, Y., Park, D.R., Suzuki, Y., Koyano, K., Tatsumi, T., *Catal. Today*, 44, 327-332 (1998)
- [17] Shioya, Y., Ikeue, K., Ogawa, M., Anpo, M., *Appl. Catal. A:General*, 254, 251-259 (2003)
- [18] Ikeue, K., Nozaki, S., Ogawa, M., Anpo, M., *Catal. Lett.*, 80, 111-114 (2002)
- [19] Tseng, I.H., Chang, W.C., Wu, J.C.S., *Appl. Catal. B:Environmental*, 37, 37-48 (2002)
- [20] Yamashita, H., Fujii, Y., Ichihashi, Y., Zhang, S.G., Ikeue, K., Park, D.R., Koyano, K., Tatsumi, T., Anpo, M., *Catal. Today*, 45, 221-227 (1998)
- [21] Solymosi, F. and Tombacz, I., *Catal. Lett.*, 27, 61-65 (1994)

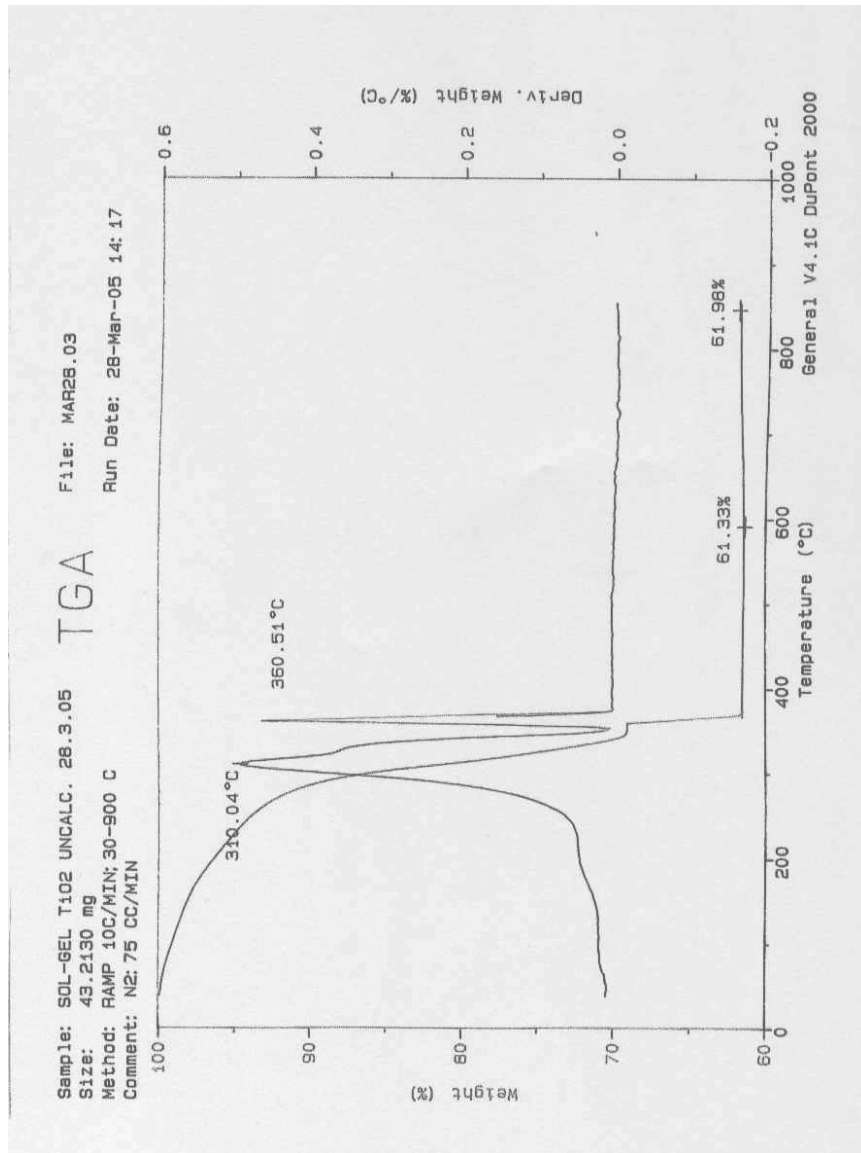
- [22] Tseng, I.H., Wu, J.C.S., *Catal. Today*, 97, 113-119 (2004)
- [23] Tseng, I.H., Wu, J.C.S., Chou, H.Y., *J. Catal.*, 221, 432-440 (2004)
- [24] Ikeue, K., Nozaki, S., Ogawa, M., Anpo, M., *Catal. Today*, 74, 241-248 (2002)
- [25] Ikeue, K., Yamashita, H., Anpo, M., *J. Phys. Chem. B*, **105**, 8350-8355 (2001)
- [26] Lin, W., Han, H., Frei, H., *J. Phys. Chem. B*, 108, 18269-18273 (2004)
- [27] Anpo, M., Takeuchi, M., *J. Catal.*, 216, 505-516 (2003)
- [28] <http://www.chemat.com/html/solgel.html> (22.06.2005)
- [29] Kim, D.J. Hahn, S.H., Oh, S.H., Kim, E.J., *Mater. Lett.*, 57, 355- 360 (2002)
- [30] Martyanov, I.N., Klabunde, K.J., *J. Catal.*, 225, 408-416 (2004)
- [31] Ichikawa, S., Doi, R., *Thin Solid Films*, 292, 130-134 (1997)
- [32] Fretwell, R., Douglas, P., *J. Photochem. Photobiol. A: Chemistry*, 143, 229-240 (2001)
- [33] Dinh, N.N., Oanh, N.Th.T., Long, P.D., Bernard, M.C., Le Goff, A.H., *Thin Solid Films*, 423, 70-76 (2003)
- [34] Kaliwoh, N., Zhang, J.Y., Boyd, I.W., *Surf. Coat. Technol.*, 125, 424-427 (2000)

- [35] Mills, A., Hill, G., Bhopal, S., Parkin, I.P., O'Neill, S.A., *J. Photochem. Photobiol. A: Chemistry*, 160, 185-194 (2003)
- [36] Takahashi, M., Tsukigi, K., Uchino, T., Yoko, T., *Thin Solid Films*, 388, 231-236 (2001)
- [37] Litter, M., *Appl. Catal. B: Environmental*, 23, 89-114 (1999)
- [38] Hao, S., Wu, J., Fan, L., Huang, Y., Lin, J., Wei, Y., *Solar Energy*, 76, 745-750 (2004)
- [39] Graetzel, M., *Prog. Photovolt. Res. Appl.*, 8, 171-185 (2000)
- [40] Snook, J.H., Samuelson, L.A., Kumar, J., Kim, Y.G., Whitten, J.E., *Org. Electron.*, 6, 55-64 (2005)
- [41] Polo, A.S., Itokazu, M.K., Iha, N.Y.M., *Coord. Chem. Rev.*, 248, 13-14, 1343-1361 (2004)
- [42] Hagfeldt, A., Grätzel, M., *Acc. Chem. Res.*, 33, 269-277 (2000)
- [43] Garcia, C.G., Lima, J.F., Murakami Iha, N.Y., *Coord. Chem. Rev.*, 196, 219-247 (2000)
- [44] Kalyanasundaram, K., Vlachopoulos, N., Krishnan, V., Monnier, A., Grätzel, M., *J. Phys. Chem.*, 91, 2342-2347, (1987)
- [45] Mao, H., Deng, H., Li, H., Shen, Y., Lu, Z., Xu, H., *J. Photochem. Photobiol. A: Chem.*, 114, 209-212 (1998)
- [47] Fan, F.-R.F., Bard, A.J., *J. Am. Chem. Soc.*, 101, 6139-6140 (1979)

- [48] Fang, J., Wu, J., Lu, X., Shen, Y., Lu, Z., Chem. Phys. Lett., 270, 145-151 (1997)
- [49] He, J.J., Hagfeldt, A., Lindquist, S.E., Grennberg, H., Korodi, F., Sun, L.C., Akermark, B. , Langmuir, 17, 2743-2747 (2001)
- [50] Funda Yükrük, PhD Thesis, Chemistry Department, Ankara, METU (2005)
- [51] Uner, D., Tapan, A., Ozen, I., Uner, M., Applied Catalysis A: General, 251, 2, 225-234 (2003)
- [52] Murat Üner, Adsorption Calorimetry in Supported Catalyst Characterization: Adsorption Sturcture Sensitivity of Pt on $\gamma\text{Al}_2\text{O}_3$, Master's Thesis Chemical Engineering Department, Ankara, METU (2004)

APPENDIX A

TGA DATA



APPENDIX B

SYNTHESIS PROCEDURES of LIGHT HARVESTING MOLECULES

The synthesis procedures for light harvesting molecules BrGly and BrAsp used in this study are given below with the intention of collecting all related information in one volume. The synthesis procedures are taken directly from the original source. [50]

B.1 Synthesis of 1,7-dibromo-3,6:9,10-perylenetetracarboxylic acid dianhydride

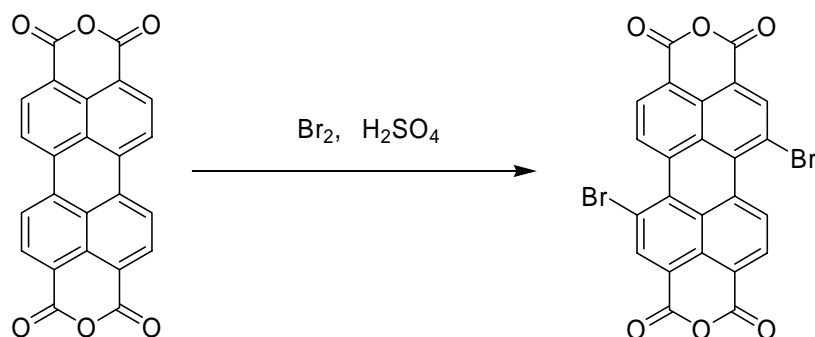


Figure B.1 Synthesis of 1,7-dibromo-3,6:9,10-perylenetetracarboxylic acid dianhydride

1,7-dibromo-3,4:9,10-perylenetetracarboxylic acid dianhydride has been prepared by the bromination of the parent anhydride. Due to very low solubility of the compound no attempt of purification was made at this stage. Therefore, some monobrominated and unbrominated compounds were present. A mixture of 1,47 g

($3,74 \times 10^{-3}$ mol perylene-3,4:9,10-tetracarboxylic acid dianhydride (>98% purity), 12,01 mL H_2SO_4 and 0,032 g I_2 were stirred for 12 hours at room temperature and then the mixture was heated to 85°C for 30 min. On cooling to room temperature, this was followed by the addition of 6.56 g (2,1 mL) Br_2 in the pressure tube during a period of 8 hours. The mixture was heated to 85°C and then followed by the addition of 9,37 g (3 mL) Br_2 during a period of 12 hours. The concentration of H_2SO_4 was decreased to 86% by adding 1,67 mL of water during 1 hour. On cooling to room temperature the precipitate was washed with g-4 glass frit and washed with 15 g H_2SO_4 (86% w/w). Then the precipitate was put into 25 mL H_2O and the mixture was stirred. The precipitate was filtered and washed with H_2O . Finally a bright-red precipitate was dried to 120°C under vacuum. Yield: 1,57 (%77)

B.2 Synthesis of 1,7-dibromo-*N,N'*-(*t*-butoxycarbonylmethyl)-3,4:9,10-perylene-diimide

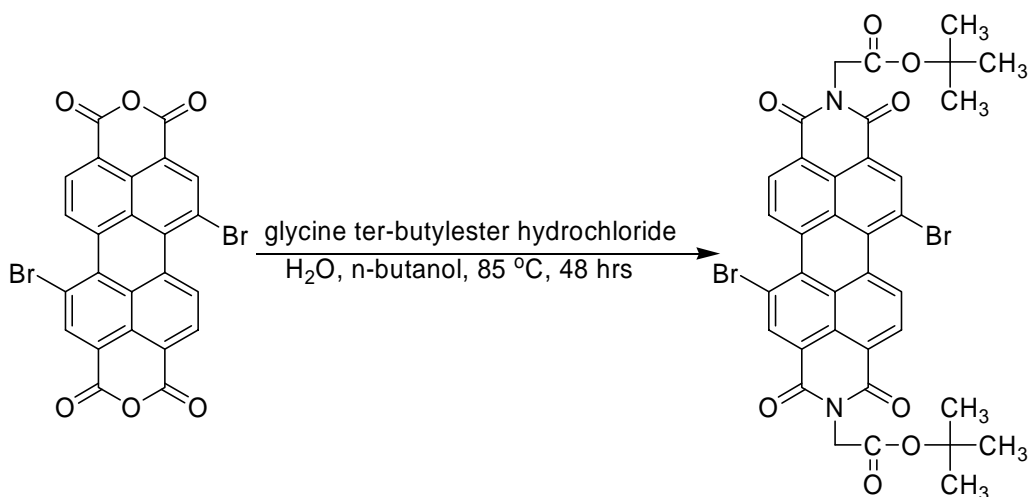


Figure B.2 Synthesis of 1,7-dibromo-*N,N'*-(*t*-butoxycarbonylmethyl)-3,4:9,10-perylene-diimide

A mixture of 1,7-dibromo-3,4:9,10-perylenetetracarboxylic acid dianhydride (0.50 g, 0.908 mmol) and glycine *t*-butylester hydrochloride (0.30 g, 1.81 mmol) in H₂O (5.0 mL), *n*-butanol (5.0 mL) and triethylamine (1.0 mL) was stirred for 48 hours at 85° C. The solvents were removed under reduced pressure. The product (reddish powder) was purified by silica gel column chromatography and preparative TLC (Solvent system: CHCl₃/MeOH 97/3) to yield 0.27 g (38%) of reddish powder, **5**. ¹H NMR (400 MHz, CDCl₃), δ (ppm) 1.45 (s, 18H, -OC₄H₉) 4.77 (s, 4H, -NCH₂), 8.65 (d, 2H, *J*=8.1 Hz, 2H), 8.86 (s, 2H), 9.41 (d, 2H, *J*=8.1 Hz). ¹³C NMR (100 MHz, CDCl₃), δ (ppm) 28.1, 42.2, 82.7, 120.7, 122.2, 122.6, 123.0, 123.3, 124.2, 128.1, 129.5, 134.6, 149.7, 162.1, 162.5, 166.6. ESI-MS (m/z); 776 [M+2H].

B.3 Synthesis of 1,7-dibromo-N,N'-(S-(1-*t*-butoxycarbonyl-2-*t*-butoxycarbonylmethyl)-ethyl)-3,4:9,10-perylenediimide

A mixture of 0.50 g (0.908 mmol) 1,7-dibromo-3,4:9,10-perylenetetracarboxylic acid dianhydride and 0.51 g (1.82 mmol) L-aspartic acid di-*t*-butyl ester in water (12.5 mL), *n*-butanol (12.5 mL) and triethylamine (2 mL) was stirred for 48 hours at 85°C. The solvents were removed under reduced pressure. The product (dark red powder) was purified by silica gel column chromatography and preparative TLC (Solvent system: CHCl₃/MeOH 99/1) to yield 0.41 g (45 %) PDI **6**. ¹H NMR (400 MHz, CDCl₃), δ (ppm) 1.33 (s, 18H, -OC₄H₉), 1.39 (s, 18H, -OC₄H₉), 2.86 (dd, 2H, *J*₁=16.2 Hz, *J*₂=7.9 Hz, -CH₂), 3.31 (dd, 2H, *J*₁=16.2 Hz, *J*₂=6.3 Hz, -CH₂), 6.05 (t, 2H, *J*=7.2 Hz, N-CH), 8.65 (d, 2H, *J*=8.2 Hz), 8.87 (s, 2H), 9.44 (d, 2H, *J*=8.2 Hz). ¹³C NMR (100 MHz, CDCl₃), δ (ppm) 27.9, 28, 29.7, 35.6, 51.1, 81.7, 82.6, 121.3, 122.3, 122.5, 123.1, 123.4, 124.4, 128.0, 129.6, 134.6, 164.4, 169.7. ESI-MS (m/z); 1002.7 [M+2H].

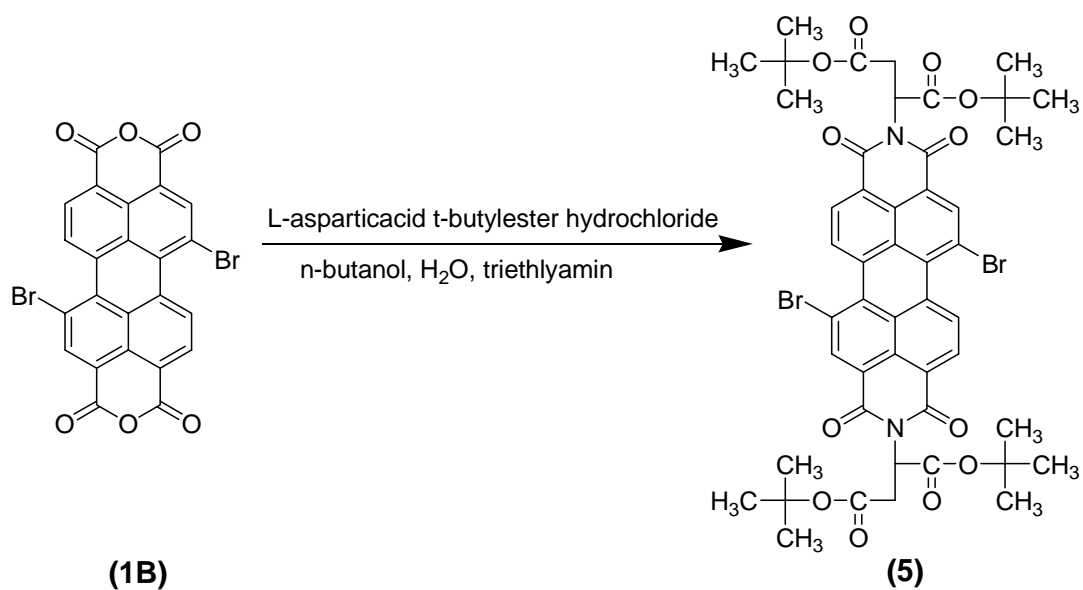


Figure B.3 Synthesis of 1,7-dibromo-N,N'-(S-(1-*t*-butoxycarbonyl-2-*t*-butoxycarbonyl-methyl)-ethyl)-3,4:9,10-perylene-3,4,9,10-perylene-3,4,9,10-dicarboxylic diimide

APPENDIX C

REACTION TEST RESULTS in TABULAR FORM

Table C.1 Thin Film Reaction Test Results

Catalyst	Light Source	Yield (micromole/grcat)			
		0 min	60 min	120 min	180 min
TiO ₂	UV	0	4.80	8.06	12.85
TiO ₂ -Pt(in)	UV	0	13.20	20.60	27.20
TiO ₂ -Pt(on)	UV	0	16.30	29.70	34.30
TiO ₂ -RuBpy	UV	0	8.70	11.60	17.50
TiO ₂ -Pt(in)-RuBpy	UV	0	25.30	39.90	43.50
TiO ₂ -Pt(in)-RuBpy	Vis	0	0.33	0.44	0.61
TiO ₂ -Pt(in)-BrGly	Vis	0	0.12	0.23	0.33
TiO ₂ -Pt(in)-BrAsp	Vis	0	0.27	0.39	0.58

Catalyst Deactivation	Yield (micromole/grcat)		
	1. Run	2. Run	3. Run
TiO ₂ -Pt(in)-RuBpy	43.5	25.7	19.0

Table C.2 Thick Film Reaction Test Results

Catalyst	Light source	Catalyst Weight (g)	Yield (micromole/grcat)			
			0 min	60 min	120 min	180 min
TiO ₂	UV	0.0359	0	3.73	5.57	7.74
	Vis	-	-	-	-	-
TiO ₂ -Pt(in)	UV	0.0535	0	7.91	11.12	14.05
	Vis	-	-	-	-	-
TiO ₂ -Pt(on)	UV	0.0292	0	11.21	17.97	25.44
	Vis	-	-	-	-	-
TiO ₂ -RuBpy	UV	0.0387	0	1.57	1.83	2.33
	Vis	0.0387	0	0.229	0.367	0.472
TiO ₂ -Pt(in)-RuBpy	UV	0.0555	0	0.901	1.151	1.607
	Vis	0.0555	0	0.148	0.336	0.446
TiO ₂ -Pt(on)-RuBpy	UV	0.0262	0	1.006	1.837	2.679
	Vis	0.0262	0	0.269	0.553	0.770
TiO ₂ -BrGly	UV	0.0288	0	0.948	1.268	2.147
	Vis	0.0288	0	0.104	0.217	0.289
TiO ₂ -Pt(in)-BrGly	UV	0.0488	0	0.495	0.829	1.108
	Vis	0.0488	0	0.106	0.200	0.299
TiO ₂ -Pt(on)-BrGly	UV	0.0264	0	1.163	1.672	2.335
	Vis	0.0264	0	0.164	0.382	0.482
TiO ₂ -BrAsp	UV	0.0345	0	0.969	1.982	2.545
	Vis	0.0345	0	0.250	0.448	0.614
TiO ₂ -Pt(in)-BrAsp	UV	0.0561	0	0.625	1.313	1.834
	Vis	0.0561	0	0.128	0.238	0.383
TiO ₂ -Pt(on)-BrAsp	UV	0.0271	0	0.953	1.927	3.366
	Vis	0.0271	0	0.295	0.529	0.757

APPENDIX D

SEM IMAGES of THIN FILMS

SEM images of thin films were taken to make sure that thin film coating is established. In SEM analysis, thin microscope glasses were used. They were coated using the same procedure as the beads. The images were taken with a JSM-6400 Electron Microscope (JEOL).

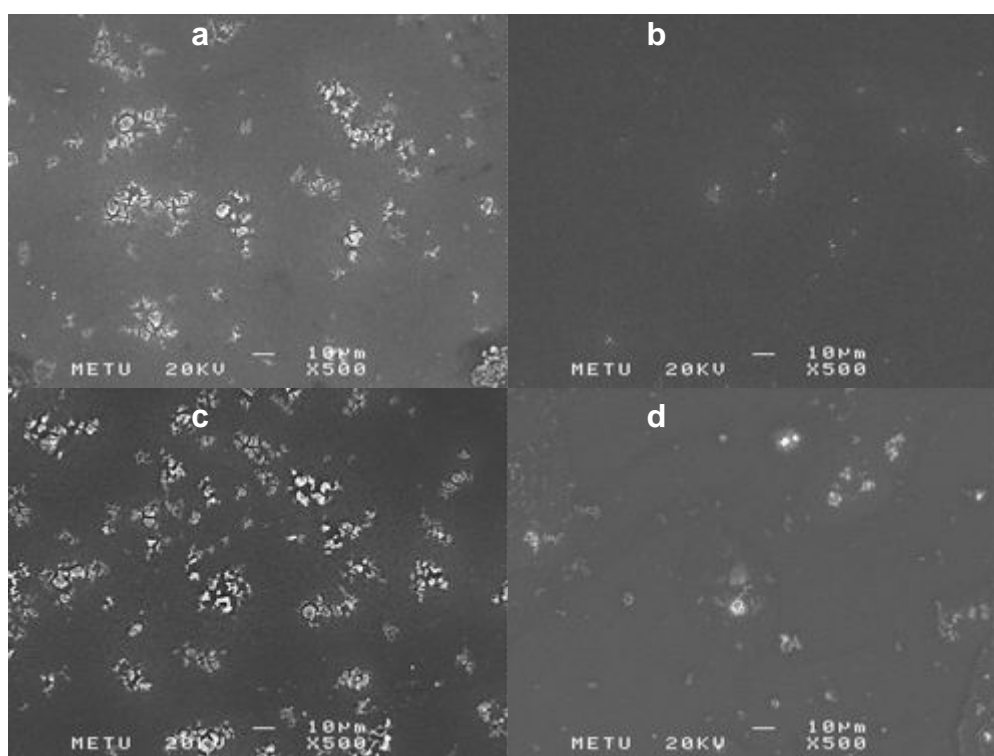


Figure D.1 SEM images of the thin films (x500)

a) TiO_2 b) $\text{RuBpy} \cdot \text{TiO}_2$ c) $\text{Pt} \cdot \text{TiO}_2$ d) $\text{RuBpy} \cdot \text{Pt} \cdot \text{TiO}_2$

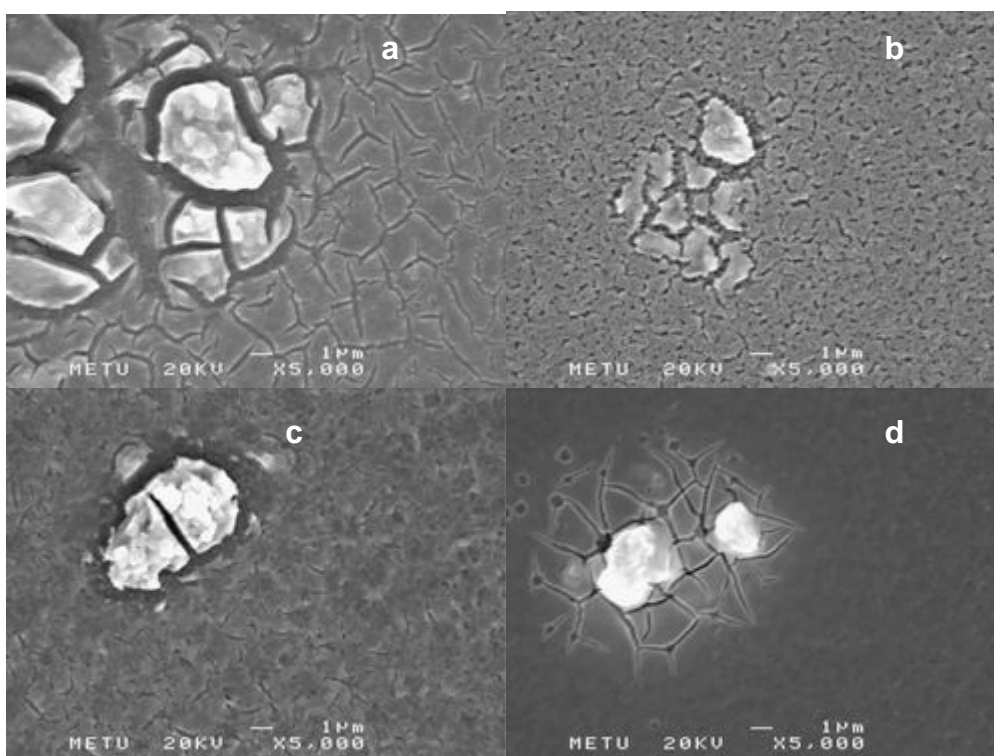


Figure D.2 SEM images of the thin films (x5000)

a) TiO_2 b) $\text{RuBpy} \cdot \text{TiO}_2$ c) $\text{Pt} \cdot \text{TiO}_2$ d) $\text{RuBpy} \cdot \text{Pt} \cdot \text{TiO}_2$

APPENDIX E

PICTURE of REACTION TEST SETUP



Figure E.1 Reaction Test Setup